OXFORD GENETICS

GENETICS, 2025, 231(1), iyaf124
https://doi.org/10.1093/genetics/iyaf124
Advance Access Publication Date: 27 June 2025
Investigation

Mutational analysis of the *Drosophila* CMG helicase reveals relationships among chromosome integrity and the maintenance of spindle and centrosome structure

Lucia Graziadio,[1] Livia Scatolini,[1] Elisabetta Bucciarelli,[2] Grazia Daniela Raffa,[1] Silvia Bonaccorsi,[1,*] Maurizio Gatti [1,2,*]

[1]Department of Biology and Biotechnology "C. Darwin", Sapienza University of Rome, Rome 00185, Italy
[2]Institute of Molecular Biology and Pathology (IBPM), National Research Council (CNR), c/o Department of Biology and Biotechnology "C. Darwin", Sapienza University of Rome, Rome 00185, Italy

*Corresponding author: Department of Biology and Biotechnology "C. Darwin", Sapienza University of Rome, Rome 00185, Italy. Email: silvia.bonaccorsi@uniroma1.it (S.B.);
*Corresponding author: Institute of Molecular Biology and Pathology (IBPM), National Research Council (CNR), c/o Department of Biology and Biotechnology "C. Darwin", Sapienza University of Rome, Rome 00185, Italy. Email: maurizio.gatti@uniroma1.it (M.G.)

The CMG (Cdc45-MCM-GINS) complex is a conserved helicase that plays an essential DNA unwinding function at replication forks. Here, we analyzed the mitotic phenotypes caused in *Drosophila* by knockdown of *Cdc45*, *Mcm5*, and the four GINS genes (*Sld5*, *Psf1*, *Psf2*, and *Psf3*). Silencing of these genes resulted in virtually identical mitotic phenotypes. Brain cells from mutant and RNAi larvae showed severe defects in chromosome condensation, chromosome breakage, and frequent polyploid mitotic figures. In addition, mutant cells showed reduced Cid (Cenp-A) incorporation at centromeres and strong alterations in spindle and centrosome structures. Our cytological and genetic analyses suggest that replication-related DNA damage and Cid-dependent centromere/kinetochore defects trigger the spindle assembly checkpoint (SAC) that arrests the cells in a prometaphase-like stage. The arrested cells undergo mitotic slippage accompanied by Cyclin B degradation and eventually return to G1 giving rise to polyploid cells. Our analyses further suggest that during the prolonged prometaphase arrest both the centrosomes and the spindles undergo severe structural degeneration and that the spindle defects are not the consequence of the aberrant centrosome behavior. Most studies on mitotic slippage have been carried out in cells exposed to anti-microtubule agents and could not address the behavior of the spindle. Conversely, our results illuminate the complex consequences of replication stress and reveal what happens to the mitotic apparatus during the prolonged spindle assembly checkpoint–induced mitotic arrest. Because prolonged mitosis is a common event in human cancers, our results could provide useful information for studies on cancer etiology and therapy.

Keywords: CMG complex; replication stress; chromosome condensation; chromosome breakage; spindle checkpoint; spindle morphology; centrosome behavior; mitotic slippage; *Drosophila*; Meier–Gorlin syndrome

Introduction

Metazoan DNA replication is a highly conserved process that involves the coordinated action of several multiprotein complexes [reviewed in Martinez *et al.* (2017), Parker *et al.* (2017), and Attali *et al.* (2021)]. The replication start sites are first bound by the hetero-hexameric Origin Recognition Complex (ORC1-6), which associates with the Cdc6 protein and the Ctd1 chaperone. The ORC-Cdc6 complex mediates the sequential recruitment of 2 MCM2-7 hexamers that encircle duplex DNA forming the prereplication complex, which is already loaded onto the DNA during the G1 phase of the cell cycle but is inactive. MCM2-7 then binds the Cdc45 protein and the GINS tetrameric complex, forming the CMG (Cdc45-MCM-GINS) protein assembly that acts as a replicative helicase, playing a DNA unwinding function at replication forks (Moyer *et al.* 2006; Ilves *et al.* 2010).

In the CMG complex, the 4 GINS proteins (Psf1, Psf2, Psf3, and Sld5, in *Drosophila*; GINS 1–4 in humans) physically interact with Cdc45 and the MCM2-7 proteins in all pairwise associations. It has been suggested that this interaction might result in allosteric changes in MCM2-7 that trigger the helicase activity of the entire complex (Ilves *et al.* 2010). It has been also reported that the GINS complex is not only necessary for initial DNA unwinding (Pacek *et al.* 2006) but also for normal progression of DNA replication (Gambus *et al.* 2006).

Several studies have shown that individual proteins of the CMG and ORC complexes are required for mitotic condensation and integrity of *Drosophila* chromosomes. Mutations in the *Orc2*, *Orc3*, and *Orc5* genes cause abnormal chromosome condensation and chromosome breakage in larval brains (Gatti and Baker 1989; Loupart *et al.* 2000; Pflumm and Botchan 2001). A similar chromosomal phenotype has been found in larval brain cells of *Mcm4* mutants (Pflumm and Botchan 2001; Crevel *et al.* 2007) and in S2 cells subjected to RNAi against either *Mcm3* or *Mcm7* (Somma *et al.* 2008). Defective chromosome condensation and chromosome fragmentation have been also observed in cultured Kc cells depleted of Orc2, Cdc45, Mcm2, or Mcm5 by RNAi (Christensen and Tye 2003). Thus, these studies collectively indicate that

Received on 15 April 2025; accepted on 19 June 2025

depletion of components of the ORC and MCM complexes disrupts chromosome condensation and integrity in *Drosophila* cells, but is currently unclear whether the observed phenotypes are fully comparable.

Studies on Cdc45 and the GINS complex proteins suggest that they might have different roles on mitotic chromosome condensation and stability. RNAi-based studies showed that the chromosomes of cells depleted of Cdc45 exhibit lateral condensation defects and breakage just like those of cells lacking Orc2, Mcm2, or Mcm5 (Christensen and Tye 2003). In contrast, the analysis of brains from larvae heterozygous for an *Sld5* null mutation revealed a defect in the longitudinal condensations of the chromosomes and frequent telomere–telomere fusions (Gouge and Christensen 2010). Abnormally elongated chromosomes were also described in brains heterozygous for a *Psf2* null mutation, but this condensation defect was not accompanied by telomeric fusions (TFs) (Chmielewski *et al.* 2012). To the best of our knowledge, the chromosomal phenotypes caused by loss of either *Psf1* or *Psf3* have never been investigated.

Cdc45 and the genes encoding the subunits of the GINS and MCM complexes are highly conserved in metazoans, and defining the phenotypic consequences of mutations in these genes in the *Drosophila* model might be relevant for human health. Indeed, the human homolog of *Psf1*, *GINS1*, is responsible for immunodeficiency 55, an autosomal recessive primary immunodeficiency characterized by intrauterine and postnatal growth retardation and lack of natural killer cells (Bernard *et al.* 2004). Mutations in the homologs of *Cdc45*, *Psf2*, and *Psf3* (*CDC45*, *GINS2*, *GINS3* in humans) cause the Meier–Gorlin syndrome (MGORS), also characterized by intrauterine and postnatal growth retardation, and microcephaly (Ting *et al.* 2020; McQuaid *et al.* 2022; Nabais Sa *et al.* 2022). Interestingly, MGORS is also caused by mutations in *ORC1*, *ORC4*, and *ORC6* (Bicknell *et al.* 2011), as well as by mutations in *MCM3*, *MCM5*, and *MCM7* (Vetro *et al.* 2017; Knapp *et al.* 2021).

The apparently inconsistent phenotypic data on the *Drosophila Psf2* and *Sld5* genes and the implication of these genes in human syndromes prompted us to reexamine the chromosomal phenotypes elicited by RNAi or mutations in *Psf2* and *Sld5*. We also analyzed the mutant and/or RNAi phenotypes of *Psf1* and *Psf3*, as well as those of *Cdc45* and *Mcm5*. We found that for all these genes the loss-of-function phenotypes in larval brain cells are virtually identical. They consist of severe defects in chromosome condensation, chromosome breakage, defects in spindle and centrosome structure, and the presence of numerous polyploid mitotic figures; we did not observe TFs in any of the mutant or RNAi animals. Our results suggest that replication-dependent DNA damage triggers the spindle assembly checkpoint (SAC) and that a prolonged SAC-mediated prometaphase arrest leads to spindle and centrosome degeneration.

Materials and methods

Fly stocks and genetics

The following mutant alleles and deficiencies were obtained from the Bloomington stock center (BDSC): $Sld5^{c01719}$ (# 85955), $Sld5^{A462}$ (# 16124), $Psf3^{A}$ (# 57119), $Psf3^{B}$ (# 57118), $Mcm5^{G3812}$ (# 63265), *Df(2L)BSC295* (#23680), and $Sas4^{s2214}$ (#12119); $Psf2^{SH0805}$ was obtained from the Kyoto Stock Center (# 122087). The $zw10^{4}$ allele (formerly $zw10^{65i20}$) is described in Williams and Goldberg (1994). For RNAi, we used the following stocks from the Bloomington and VDRC collections: *Sld5* (BDSC # 54047), *Psf1* (v10229), *Psf2* (v33040), *Psf3* (v20849), *Mcm5* (BDSC # 41871), and *Cdc45* (v110478). In all cases, expression of the UAS-RNAi construct was induced with an Actin-GAL4 driver (BDSC # 4414). We note that larvae bearing the *Psf3* (v20849) RNAi construct and the Actin-GAL4 driver are viable and that their brains do not show mitotic defects. In contrast, *Sld5*, *Psf1*, *Psf2*, *Mcm5*, and *Cdc45* RNAi larvae are lethal and their brains display frequent mitotic aberrations. Mutations and insertions on the second and third chromosome were maintained in stock using the *CyO-TbA* (Lattao *et al.* 2011) and *TM6B* balancers, both carrying the larval marker *Tubby (Tb)*. X chromosome-linked mutations were kept either over the *FM7-GFP* or the *FM7-TbA* balancer (Lattao *et al.* 2011). To obtain $Psf2^{SH0805}/Df$ larvae, we crossed $Psf2^{SH0805}$/CyO-*Tb*A to *Df(2L)BSC295/CyO-TbA* flies and selected third instar larvae for the non-Tb phenotype. All flies were reared according to standard procedures and maintained at 25°C. The genetic markers and special chromosomes are described in detail in FlyBase (http://www.flybase.org).

Cytology and immunofluorescence

For immunostaining, larval brains were dissected in saline (0.7% NaCl) and fixed for 20 min in 3.7% formaldehyde according to Bonaccorsi *et al.* (2000). After several rinses in PBS, slides were incubated overnight with different combinations of the following primary antibodies diluted in PBS: monoclonal anti-alpha tubulin (1:1,000; Sigma Aldrich); monoclonal anti-γ tubulin (1:50; Sigma-Aldrich); mouse anti-γH2Av (1:20;DSHB); rabbit anti-DSpd-2 (1:3,000; Giansanti *et al.* 2008); rabbit anti-phospho-Histone3 (PHH3; 1:250; EMD Millipore Corporation); rabbit anti-Cyclin B (Cyc B; 1:100; Lehner and O'Farrell 1990); and chicken anti-Cid (1:5000; Blower and Karpen 2001). Primary antibodies were detected by 1-h incubation at room temperature with FITC-conjugated anti-mouse IgGs (1:20; Jackson Laboratories), CY3-conjugated anti-rabbit IgG (1:300; Invitrogen), Cy3-conjugated anti-mouse IgGs (1:50, Jackson Laboratories), and Cy3-conjugated anti-chicken IgGs (1:50, Jackson Laboratories), all diluted in PBS. Immunostained preparations were mounted in Vectashield H-200 with DAPI (Vector Laboratories).

The mitotic index (MI) was calculated by determining the average number of mitotic figures per optic field (100× Nikon objective) as described by Gatti and Baker (1989). The MIs reported in the figures are the averages from at least 3 brains.

To analyze the morphology and integrity of metaphase chromosomes, brains from third instar larvae were dissected in saline (NaCl 0.7%), incubated for 1 h with colchicine (10^{-5}M in saline), treated for 10 min with hypotonic solution (0.5% Na Citrate), squashed in 45% acetic acid, and immediately frozen in liquid nitrogen. After flipping of the coverslip, squashed brains were mounted in Vectashield H-200 with DAPI (Vector Laboratories).

Microscopy

All cytological preparations, except those stained for either Cid or γH2Av, were examined using a Nikon Eclipse F600, equipped with a CCD camera (Photometrics CoolSnap MYO). Grayscale images were collected separately, pseudocolored, and merged. Cyc B fluorescence of mitotic cells was measured on photographs using the Image J software. Prometaphases were considered Cyc B-positive if their fluorescence intensity (number of pixels per unit area) was at least 2 times higher than that of neighboring interphase cells. Cid- and γH2Av-stained slides were examined using a Zeiss Axioplan fluorescence microscope equipped with an Axiocam 512 (Zeiss) monochromatic camera. γH2Av and Cid signals were quantified using Zen 2.5 Pro software (Zeiss, Germany). Image z-stacks were acquired using an Axiocam 512

(Zeiss) camera. Signals were considered positive starting from 3 times the basal fluorescence.

qRT-PCR measurements of mRNA levels

RNA was extracted with the TRIzol reagent (Ambion), treated with RNase-free TM DNase I (Ambion), and then purified using a standard phenol/chloroform protocol. One microgram of intact RNA was reverse transcribed using RevertAid H Minus First Strand cDNA Synthesis Kit (Thermo Scientific, EP0451) with random hexamers. Real-time PCR reactions were carried out using the SensiFASTTM SYBR No-ROX Kit, with QuantStudioTM 3 Real-Time PCR System. Relative quantification of gene expression was carried out using the 2−ΔΔCt method and the *Rp49* gene for normalization. PCR data are from 3 biological replicates obtained using the primer pairs described in Supplementary Table 1.

Results

Mutations in *Sld5* affect chromosome and spindle structure but not telomere stability

To define the phenotypes associated with loss of the GINS complex activity, we first analyzed mutants in the *Sld5* gene. We used 2 mutant alleles obtained from the Bloomington stock center, $Sld5^{c01719}$ and $Sld5^{A462}$. Both alleles carry PBac elements inserted in identical positions in the second exon of the gene and are predicted to lead to truncated gene products. Previous work reported that flies homozygous for either $Sld5^{c01719}$ or $Sld5^{A462}$ die as embryos/first instar larvae and that $Sld5^{c010719}$/+ and $Sld5^{A462}$/+ heterozygotes are viable but show frequent TFs (Gouge and Christensen 2010). We first investigated whether indeed heterozygosity for $Sld5^{c010719}$ or $Sld5^{A462}$ leads to the formation of TFs. To this end, larval brains were incubated in saline supplemented with colchicine, subjected to hypotonic treatment, and then fixed and stained with DAPI (see Materials and methods for details). Our previous work showed that this procedure yields well-spread metaphase chromosomes, which allow a reliable assessment of the presence of TFs [see for example Cenci *et al.* (1997, 2003)]. We examined the chromosomal phenotype of larval brains heterozygous for each of these 2 *Sld5* mutations, but did not detect any TFs (200 cells scored from 3 brains in each heterozygous combination).

We confirmed that $Sld5^{c01719}$ homozygotes and $Sld5^{c01719}$/*Df(3R)BSC495* hemizygotes die as embryos/first instar larvae (Gouge and Christensen 2010). However, in contrast with previous work (Gouge and Christensen 2010), an examination of $Sld5^{A462}$/*TM6B* culture tubes revealed the presence of some third instar homozygous mutant larvae, which were easily recognized for their non-*Tubby* phenotype. Brain squashes from these mutant larvae were stained for both DNA and the phosphorylated histone variant H2Av (γH2Av; the *Drosophila* homolog of mammalian H2AX), a marker for defective DNA replication and the consequent DNA damage (Andreyeva *et al.* 2008; Fragkos *et al.* 2023). The nuclei of *Sld5* mutant brains exhibited a 3-fold increase in γH2Av foci compared to control, suggesting that they had been subjected to high replication stress (Supplementary Fig. 1).

To analyze mitosis, *Sld5* mutant brains were stained for DNA, tubulin, and the anti-phospho-histone H3 antibody (PHH3) that marks mitotic chromatin (Wei *et al.* 1999). In mutant brains, most dividing cells were arrested in a prometaphase-like stage with disorganized spindles; metaphases with aligned chromosomes were much less frequent than in controls (2.3% vs 17.2%; Fig. 1a and d), while anaphases and telophases were virtually absent (0.9% vs 20.3%; Fig. 1d). In addition, in mutant brains, most mitotic cells displayed irregular chromosome condensation and frequent chromosome fragmentation (Fig. 1a–c); in some PHH3-positive cells, chromatin condensation was so abnormal that individual chromosomes were not recognizable (Fig. 1a–c). Finally, a large fraction (43.5%) of mutant cells were clearly hyperploid/polyploid (Fig. 1c–e).

Importantly, the spindles of most (87.2%) prometaphase cells were severely defective ranging from completely unstructured microtubule assemblies to morphologically irregular spindle-like structures (Fig. 1a and e). We define as morphologically irregular spindles those that have a bipolar structure but exhibit irregularities in the poles and/or structural differences between the 2 halves of the spindle (see examples in Fig. 1). Eighty-two percent of polyploid prometaphase-like figures also displayed completely disorganized spindles (Fig. 1c and e). Of note, some unstructured prometaphase spindles were present also in controls, although at a much lower frequency than in the mutant (15.8% vs 65.4%; these frequencies are relative to the number of diploid prometaphases). We believe that most of the control spindles we classified as "unstructured" are in fact perfectly normal spindles. They are usually relatively small spindles with MTs arranged in a star-like configuration. Most likely these spindles result from a squashing pressure applied in the same direction of spindle axis.

Mutant brains also showed a few diploid prometaphase-like cells with elongated spindles (PMLES; Fig. 1b and e). PMLES have been previously observed in S2 cells with centromere/kinetochore defects. They contain chromosomes comprised of both sister chromatids and high levels of Cyclin B, but are associated with elongated anaphase-like spindles (Somma *et al.* 2008; Renda *et al.* 2017; Pellacani *et al.* 2018; Pavlova *et al.* 2019). Thus, PMLES are prometaphase cells that are nevertheless undergoing spindle elongation as it normally occurs during anaphase.

Of note, the spindles of the *Sld5* and the other mutants shown in Fig. 1 have different sizes. This is because *Drosophila* larval brains contain different types of dividing cells: type I neuroblasts (NBs) that divide asymmetrically generating another type I NB and a smaller ganglion mother cell (GMC) and type II NBs that divide asymmetrically producing another type II NB and an intermediate precursor (INP) cell, which also divides asymmetrically several times giving rise to INPs and a GMCs. GMCs divide symmetrically only once producing daughter cells that will differentiate in neurons or glial cells (Homem and Knoblich 2012). Although to the best of our knowledge the spindle sizes of these types of dividing cells have never been accurately measured, they are likely to be quite different, as suggested by the images shown in Supplementary Fig. 2. Our overall observations strongly suggest that in *Sld5* and the other mutants examined, here all spindles are affected regardless of their size.

To further define the chromosomal phenotype of homozygous *Sld5* mutants, we treated the brains with colchicine for 1 h and then subjected them to hypotonic treatment and fixation with acetic acid (see Materials and methods). This procedure allows a clear visualization of the chromosomes and a reliable assessment of chromosome integrity and condensation as well as chromosome number. Analysis of preparations revealed that nearly all cells with an apparently diploid chromosome complement exhibit irregularly condensed and/or broken chromosomes (Fig. 2a and b). We also confirmed that approximately one half of the mitotic figures in mutant brains are hyperploid/polyploid (Fig. 2b). We did not observe any clear case of telomere–telomere fusion.

The discrepancy between our study and previous work about the presence of TFs in *Sld5* mutant brains is notable. We used the same mutant alleles used by Gouge and Christensen (2010)

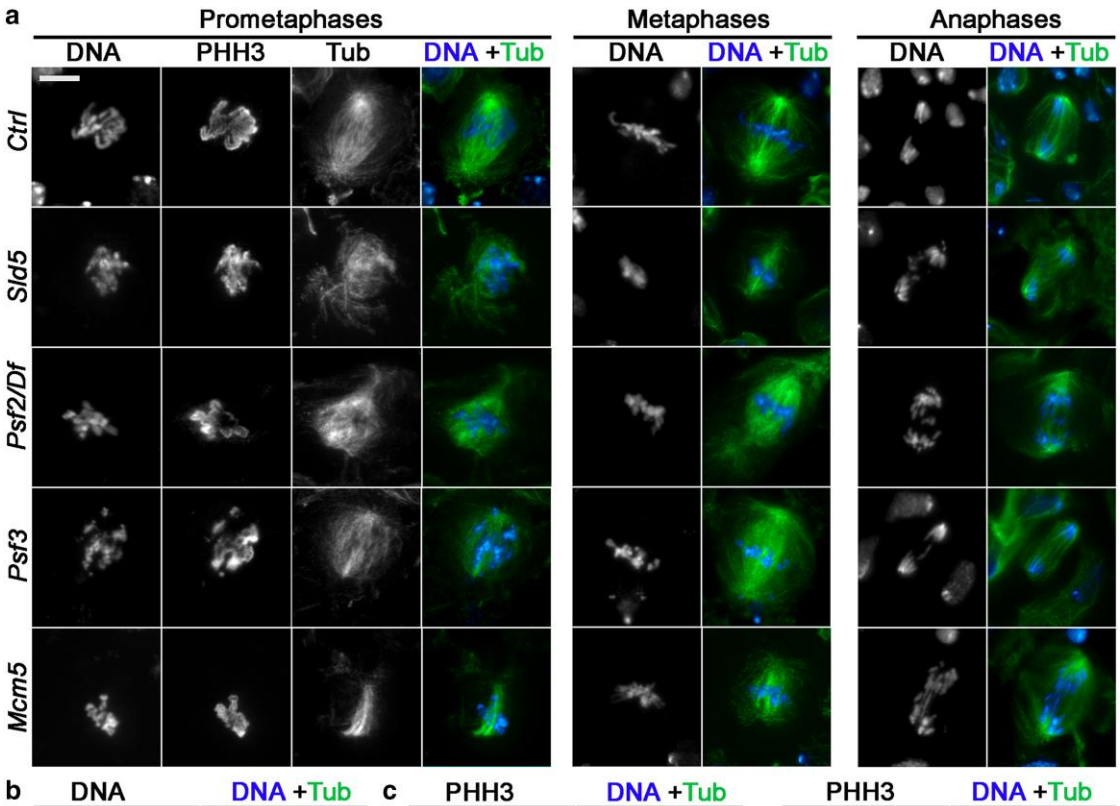

d

Mutant	# of brains/MI	# of cells	Diploid % (1)					Poly % (2)
			PM R	PM C/B	Tot. PM	Meta	Ana-telo	
Ctrl	9/1.90	985	62.2	0.3	62.5	17.2	20.3	0.1
Sld5	13/0.80	391	3.6	93.2	96.8	2.3	0.9	43.5
Psf2/Df	8/3.17	745	9.9	83.2	93.1	6.0	0.9	26.6
Psf3	10/2.52	533	5.1	86.7	91.8	6.1	2.1	29.6
Mcm5	12/1.10	587	4.2	90.4	94.6	2.7	2.7	42.8

e

Mutant	# brains/ # cells	Diploid									Polyploid		
		Prometaphases					Metaphases		Ana-telo				
		R	IR	PL	U	Ab%	R	IR	R	IR	R	IR	U
Ctrl	5/403	163	34	0	37	30.3	76	3	87	3	0	0	0
Sld5	9/223	10	29	7	87	87.2	4	1	1	1	4	11	68
Psf2/Df	4/282	65	62	17	63	60.4	13	1	3	3	8	13	34
Psf3	6/354	54	66	11	120	74.1	17	3	2	2	8	14	57
Mcm5	8/337	41	40	16	120	73.7	6	1	8	2	14	6	83

Fig. 1. Mutations in the CMG complex genes affect mitotic chromosome condensation and integrity and disrupt spindle organization. a) Mitotic phenotype of diploid cells of noncolchicine, nonhypotonic-treated brains from control (*Ctrl*, mutant/balancer), *Sld5*, *Psf2/Df*, *Psf3*, and *Mcm5* mutant larvae. Cells were immunostained for tubulin (Tub) and the mitotic marker phospho-histone H3 (PHH3) and counterstained with DAPI. Prometaphase chromosomes of all mutants show defects in condensation and integrity. The *Sld5* and *Psf2/Df* PMs shown in this figure exhibit "unstructured" spindles, while *Psf3* and *Mcm5* PMs have irregularly shaped (IR) spindles. Metaphase spindles are morphologically regular; anaphase spindles are also regular but show lagging chromosome fragments. b) Examples of PMLES with regular spindles. c) Examples of polyploid cells with unstructured spindles [see text for detailed explanations on a)–c)]. Scale bar, 10 μm. d) Quantification of the mitotic parameters of mutant brain cells. MI, mitotic index; see Materials and methods for MI calculation; PM, prometaphases; Meta, metaphases; Ana-telo, ana-telophases; R, regular; C/B, chromosome breakage and/or defective chromosome condensation; Poly, polyploid cells. (1) Percentages from diploid cells only. (2) Percentage from total cells scored. e) Quantification of defects in spindle morphology observed in brains of mutant larvae. R, regular; IR, irregular; PL, PMLES; U, unstructured spindles; Ab %, percent of diploid PMs with abnormal spindles, IR and U, but not PL have been considered abnormal. The frequencies of PM C/B, Tot PM, metaphases, ana-telophases, and polyploid cells d) and the frequencies of abnormal PM spindles (Ab) e) observed in the mutants are all significantly different from controls ($P < 0.0001$, χ^2 contingency test).

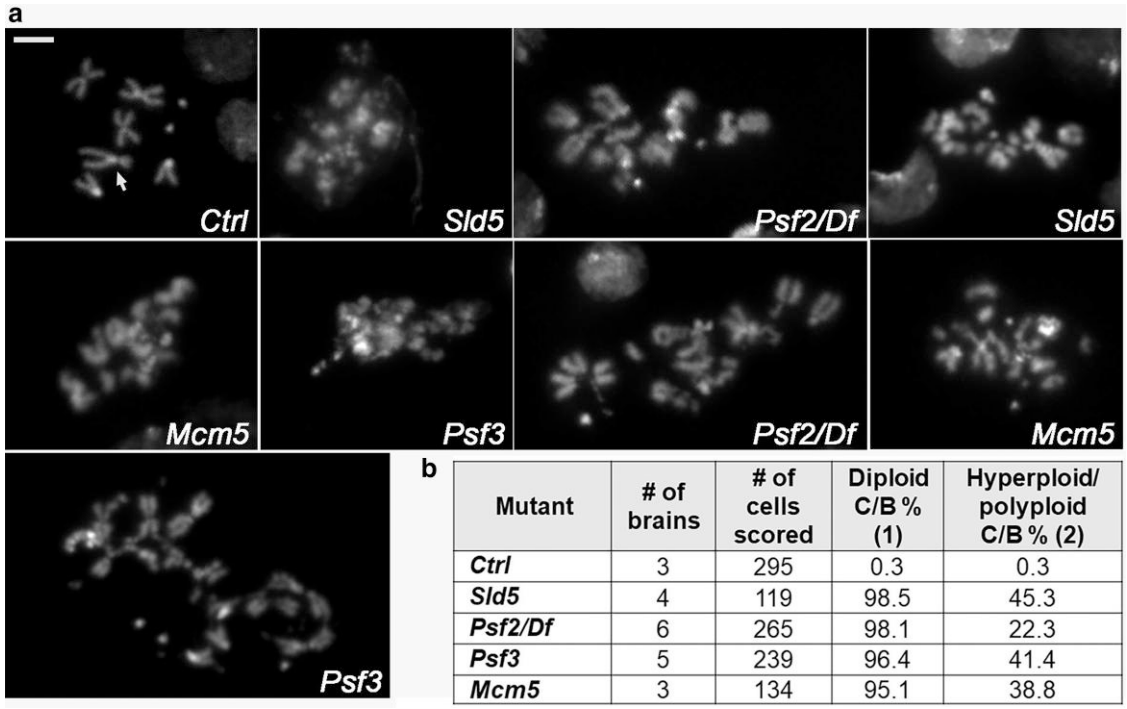

b

Mutant	# of brains	# of cells scored	Diploid C/B % (1)	Hyperploid/ polyploid C/B % (2)
Ctrl	3	295	0.3	0.3
Sld5	4	119	98.5	45.3
Psf2/Df	6	265	98.1	22.3
Psf3	5	239	96.4	41.4
Mcm5	3	134	95.1	38.8

Fig. 2. Mutations in the CMG genes result in defective chromosome condensation and chromosome aberrations (CABs). a) Examples of metaphases from colchicine-treated brains (c-metaphases) of control (Ctrl, mutant/balancer), *Sld5*, *Psf2*, *Psf3*, and *Mcm5* mutants. Cells were hypotonically swollen, fixed, and stained with DAPI. The c-metaphases show defective chromosome condensation and CABs. The control cell (*Ctrl*) carries the *Sdl5* mutation balanced over TM6B, which has a submetacentric structure (arrow). The *Psf3* mutant cell at the bottom is tetraploid and exhibits multiple chromatid exchanges and breaks. Scale bar, 5 μm. b) Quantification of cells with defective chromosome condensation and/or CABs (C/B), and hyperploid/polyploid cells. (1) Percentages from diploid cells only. (2) Percentage from total cells scored; all polyploid cells showed defects in chromosome condensation and integrity. The frequencies of C/B diploid cells and hyperploid/polyploid cells observed in mutant brains are both significantly different from those of control ($P < 0.0001$, χ^2 contingency test).

and did not see any TF in both heterozygous and homozygous *Sld5* brains. In addition, we did not see TFs in *Sld5* RNAi brains (see below). We believe this discrepancy is at least in part related to the fact that we examined colchicine-treated brains where TFs are easily recognizable, while Gouge and Christensen (2010) scored noncolchicine-treated brain squashes, where images are often unclear and difficult to interpret.

Mutations in *Psf2* and *Psf3* result in mitotic phenotypes very similar to those elicited by *Sld5* mutations

To ascertain whether the mitotic phenotypes caused by *Sld5* mutations were a specific outcome of the knockout of this gene or were instead a general consequence of GINS complex inactivation, we also analyzed the loss-of-function phenotypes of *Psf2* and *Psf3*. We did not examine *Psf1* mutants, as no mutations in this gene were available in the Stock Centers.

We obtained 2 *Psf3* mutant alleles from the Bloomington stock center: $Psf3^A$ and $Psf3^B$. $Psf3^A$ carries a lethal missense mutation (FlyBase); $Psf3^B$ carries a G>A nucleotide change that results in a premature stop codon (FlyBase). Both $Psf3^A$ and $Psf3^B$ were balanced over *FM7-GFP*; $Psf3^A$/*FM7-GFP* and $Psf3^B$/*FM7-GFP* females produced $Psf3^A$/Y and $Psf3^B$/Y third instar male larvae that never reached the adulthood. Analysis of fixed larval brains stained for DNA, tubulin, and PHH3 revealed that the 2 mutations cause comparable mitotic phenotypes. We focused on $Psf3^A$ because the $Psf3^A$/*FM7-GFP* stock was healthier than $Psf3^B$/*FM7-GFP*. γH2Av staining revealed that the $Psf3^A$ mutant brains exhibit a ~3-fold increase in γH2Av nuclear foci compared to control, indicating that they had been subjected to a replication stress similar to that suffered by the *Sld5* mutant brains (Supplementary Fig. 1).

For the phenotypic analysis of *Psf2* mutants, we used the $Psf2^{SH0805}$ allele that carries a P-element insertion in the second exon of the gene. Previous work reported that flies homozygous for $Psf2^{SH0805}$ die as embryos/first instar larvae, while $Psf2^{SH0805}$/+ heterozygotes are viable but show defective longitudinal condensation of the chromosomes (Chmielewski *et al.* 2012). We found that $Psf2^{SH0805}$/+ heterozygotes are fully viable and fertile but we were not able to detect the presence of gross defects in chromosome condensation in their larval brains. We confirmed that $Psf2^{SH0805}$ homozygous mutant larvae do not reach the third instar stage. However, we were able to isolate some $Psf2^{SH0805}$/*Df(2L)BSC295* (henceforth *Psf2/Df*) hemizygous third instar larvae.

The brains of $Psf3^A$/Y and $Psf2^{SH0805}$/*Df* larvae displayed strong mitotic defects extremely similar to those seen in homozygous *Sld5* mutants: an abundance of prometaphase-like figures with disorganized spindles, very low frequencies of metaphases and anaphases/telophases, and many hyperploid/polyploid prometaphase-like figures (Fig. 1a–e). Nearly all dividing cells also showed defects in chromosome condensation ranging from cells with moderately swollen chromosomes to cells where the individual chromosome morphology was no longer distinguishable (Fig. 1a–e). Also in colchicine-treated brains of *Psf3* and *Psf2* mutants, we observed a chromosomal phenotype very similar to that seen in *Sld5* mutants, consisting in combinations of 3 phenotypic traits: irregularly condensed chromosomes, broken chromosomes, and hyperploid/polyploid figures (Fig. 2a and b).

The *Mcm5* knockout phenotype is fully comparable to those observed in mutants for the GINS genes

The common phenotypes observed in the GINS mutants led us to wonder whether they reflect a specific role of this subcomplex, or whether they are a general consequence of the replication stress caused by loss of the CMG helicase activity. To address this question, we examined the phenotype caused by mutations in *Mcm5* that encodes another component of CMG complex.

Previous work showed that larval brain cells from *Mcm4* mutants exhibit abnormal chromosome condensation and chromosome breakage (Pflumm and Botchan 2001). RNAi against *Mcm2* or *Mcm5* in Kc tissue culture cells also resulted in chromosomes with defective lateral condensation and chromosome fragmentation (Christensen and Tye 2003), and a similar phenotype was observed in S2 cells depleted of either Mcm3 or Mcm7 by RNAi (Somma *et al.* 2008). Here, we focused on the effects of *Mcm5* mutations in larval brains, a phenotypic analysis not previously performed. We analyzed the effects of the $Mcm5^{G3812}$ mutation that carries a P{EP} element inserted into the first exon of the gene. Flies homozygous for $Mcm5^{G3812}$ were lethal but some mutant larvae survived till third instar, allowing cytological analysis. Here again, we stained $Mcm5^{G3812}$ mutant brains for γH2Av and found that they exhibit a ∼3-fold increase in foci compared to controls, similarly to the *Sld5* and *Psf3* mutant brains (Supplementary Fig. 1). Consistent with these results, brains from $Mcm5^{G3812}$ homozygotes stained for DNA, PHH3, and tubulin displayed a mitotic phenotype indistinguishable from that observed in *Sld5*, *Psf2*, and *Psf3* mutants (Fig. 1). In addition, colchicine-treated $Mcm5^{G3812}$ mutant brains showed abnormally condensed and broken chromosomes just as those observed in brains from of *Sld5*, *Psf2*, and *Psf3* mutants (Fig. 2).

RNAi against *Psf1*, *Ccd45*, *Mcm5*, *Sld5*, or *Psf2* results in similar mitotic phenotypes

To expand our cytological analyses of the consequences of the CMG complex inactivation, we decided to examine the loss-of-function phenotype of the *Psf1* and *Cdc45* genes, for which no mutations were available. We thus performed RNAi against these genes in living flies and analyzed the resulting mitotic phenotype in larval brains. For comparison, we also analyzed RNAi brains for *Sld5*, *Psf2*, or *Mcm5*. We generated flies bearing an appropriate RNAi construct and the actin-GAL4 driver. All these flies died at the larval/pupal stage allowing cytological analysis of larval brain mitotic phenotype. qRT-PCR analysis of RNAi larval brains revealed substantial decreases in the *Sld5*, *Psf1*, *Psf2*, *Mcm5*, and *Cdc45* mRNAs levels compared to control (Supplementary Fig. 3).

Preparations from all RNAi brains displayed mitotic defects that were qualitatively similar to those of the mutants, although they were milder and more variable in intensity (Supplementary Fig. 4a–d). For example, in all cases, the frequency of cells in prometaphase was significantly higher than in wild-type controls, while the frequencies of metaphases and anaphases were significantly lower than in controls (Supplementary Fig. 4c). In addition, mitotic cells from all RNAi brains displayed the same types of spindle defects as those seen in the mutants (Fig. 1; Supplementary Fig. 4a and d).

Preparations from colchicine-treated RNAi brains also displayed chromosomal phenotypes comparable to those observed in the mutants. In all cases, in addition to cells showing normal or almost normal chromosome condensation, we observed cells with irregularly condensed and broken chromosomes (Supplementary Fig. 5a and b), but we never found TFs. In contrast with the mutant brains, in which most cells have multiple breaks, several cells in RNAi brains showed a limited number of breaks, allowing mapping of the breakpoints along the chromosomes. The analysis of diploid cells with normal or almost normal chromosome condensation revealed that in *Sld5*, *Psf1*, *Psf2*, *Ccd45*, and *Mcm5* RNAi brains the isochromatid breaks (chromosome breaks involving both sister chromatids at the same locus) are preferentially located in the heterochromatin or at the junction between euchromatin and heterochromatin (henceforth, we designate both as heterochromatic breaks) (Supplementary Fig. 5a and c). Previous studies showed that X-ray-treated wild-type cells and mutants in *mei-9* and *mei-41* display 40–50% heterochromatic breaks, while mutants in *mus-109* exhibit 81% heterochromatic breaks (Gatti *et al.* 1974; Gatti 1979; Baker *et al.* 1982) (see Supplementary Fig. 5c). *mei-9* and *mei-41* encode proteins homologous to the ERCC endonuclease and the ATR kinase, respectively [reviewed by Sekelsky (2017)] while *mus-109* encodes the *Drosophila* ortholog of the highly conserved DNA2 helicase/nuclease (Mitchell *et al.* 2022). These data and our current results collectively suggest that *Drosophila* heterochromatin is particularly sensitive to DNA damage induced by replication stress.

As a whole, our analyses indicate that the *Psf1* and *Cdc45* RNAi phenotypes are very similar to those induced by RNAi against *Sld5*, *Psf2*, or *Mcm5*. This suggests that all these phenotypes are caused by the same primary DNA replication defect due to reduced CMG helicase activity.

Mutations in *Sld5*, *Psf3*, and *Mcm5* cause centrosome defects in larval brain cells

We have shown that silencing of genes that encode components of the CMG complex results in highly abnormal spindles. However, the mechanisms underlying the formation of these spindles are unclear. To address this issue, we focused on *Sld5*, *Psf3*, and *Mcm5* mutants, which exhibit the highest frequencies of both defective spindles and hyperploid/polyploid figures in larval brains. Because previous work on mammalian cells showed that the SLD5 and MCM5 proteins localize to the centrosomes and affect centrosome structure and/or behavior (Ferguson and Maller 2008; Kaur *et al.* 2018), we first analyzed mutant brains for centrosome integrity and number. *Sld5*, *Psf3*, and *Mcm5* mutant brains were fixed and stained for DNA, tubulin, and the Spd2 centrosomal marker (Giansanti *et al.* 2008). Spd2 is a highly conserved centrosomal component, which forms a scaffold-like structure that recruits the pericentriolar material (PCM) and is therefore required for MT nucleation (Conduit *et al.* 2014). In control brains stained for Spd2, 98.5% of mitotic cells ($n = 214$) showed 2 centrosomes, cells with a single centrosome were only 1.5%, and cells without centrosomes were not observed. In contrast, in mutant brains, most diploid mitotic cells displayed centrosome aberrations (Fig. 3). Importantly, these aberrations were qualitatively similar in the 3 mutants examined. In diploid cells, the most frequent defect was the complete absence of detectable centrosomes (Fig. 3a and c; Supplementary Table 2). We also observed cells with a single centrosome, which was usually larger than a normal centrosome and often showed a noncompact and granular appearance (Fig. 3a and b; Supplementary Table 2). In addition, some of the diploid cells devoid of organized centrosomes or with a single centrosome displayed several Spd2 positive granules, suggesting that the PCM was disintegrating (Fig. 3a). Finally, about 30% of hyperploid/polyploid cells were not associated with any recognizable centrosome, while 30–40% of these cells displayed

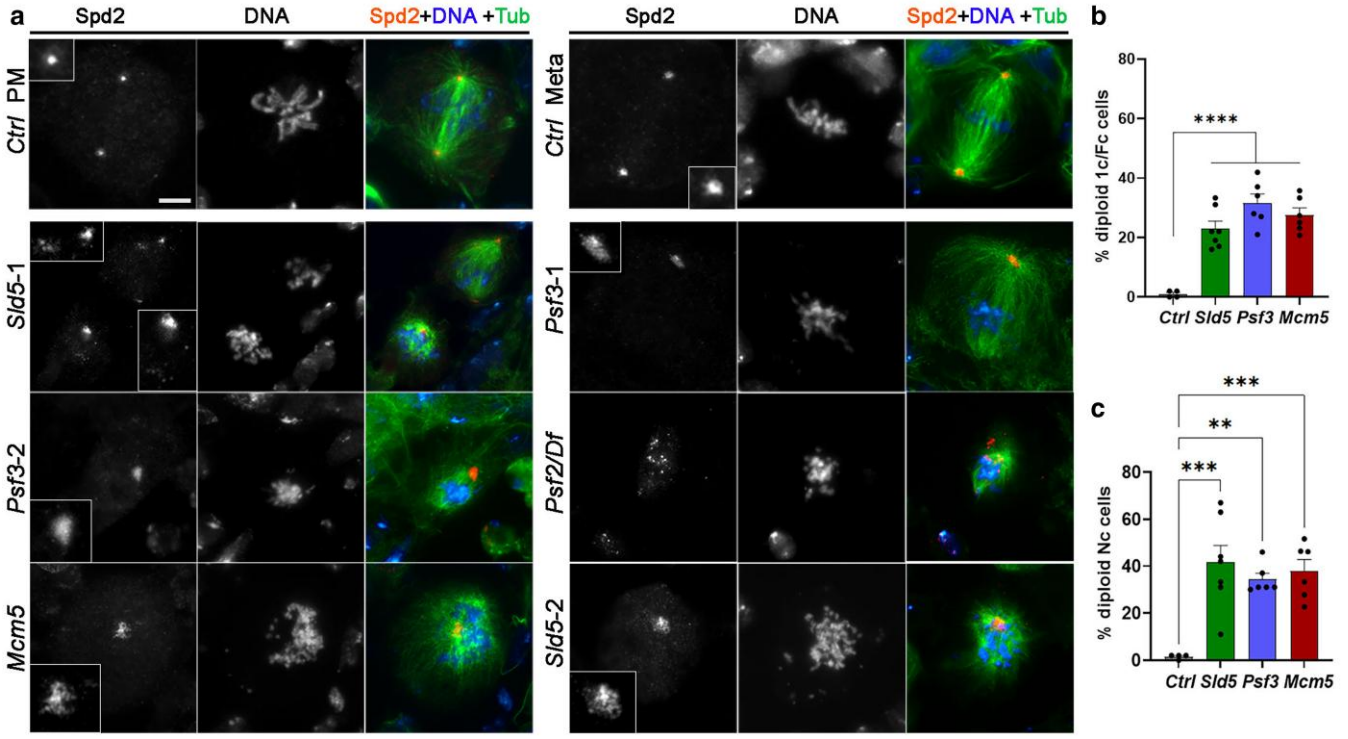

Fig. 3. Mutations in the CMG genes cause centrosome aberrations. a) Examples of centrosome aberrations found in CMG mutants. Noncolchicine, nonhypotonic-treated brain squashes were immunostained for the centrosome marker Spd2, tubulin, and counterstained with DAPI. *Ctrl* PM, *Ctrl* Meta, and insets: control prometaphase and metaphase showing compact centrosomes; *Sld5*-1 and insets: 2 diploid PMs showing partial centrosome fragmentation; *Psf3*-1 and inset: PM with a single noncompact centrosome with MT nucleation ability; *Psf3*-2: diploid PM with a single centrosome with no apparent MT nucleation ability; *Psf2/Df*: diploid PM showing centrosome fragmentation; *Mcm5*, *Sld5*-2 and insets: polyploid cells showing a single noncompact centrosome with no apparent MT nucleation ability. Scale bar, 5 μm. b and c) Frequencies of diploid mitotic cells (±SEM) with a single and/or fragmented centrosome (1c/Fc; b), or devoid of centrosomes (Nc, c). The dots represent frequencies observed in individual brains from 3 different experiments. Significance was assessed by ANOVA and Tukey multiple comparison; ****, ***, and **: $P < 0.0001$, 0.001, and 0.01, respectively. See Supplementary Table 2 for detailed information on centrosome and spindle structure.

fragmented centrosomes or a single large and noncompact centrosome (Fig. 3a, bottom panels; Supplementary Table 2). In both diploid and polyploid cells, the centrosome fragments and many of the single, and often large, centrosomes did not show any clear MT nucleating activity. Immunostaining for both Spd2 and γ-tubulin revealed that the 2 types of centrosomal signals were both present and overlapping in virtually all cells (at least 50 dividing cells examined per mutant). Based on these observations, we hypothesize that the centrosomes of both diploid and polyploid cells arrested in prometaphase undergo a degeneration process that starts with centriole disengagement (Karki *et al.* 2017; Wilhelm *et al.* 2019) and PCM fragmentation and might end up with complete centrosome disappearance. We further speculate that when only one of the 2 centrosomes disintegrates, the resulting fragments can associate with the remaining centrosome, leading to the formation of an enlarged centrosome.

Mutations in *Sld5*, *Psf3*, and *Mcm5* mutants affect Cid recruitment at centromeres and trigger the SAC

Our results clearly show that mutations in *Sld5*, *Psf3*, or *Mcm5* lead to an arrest of mitotic cells in prometaphase, suggesting that these cells might be unable to satisfy the SAC. This result is not surprising as previous work has shown that DNA damage and/or replication stress trigger the SAC. There is also ample evidence that the DNA damage response (DDR) and the SAC proteins interact and cooperate to prevent cells from entering anaphase (Su 2011; Luna-Maldonado *et al.* 2021). Previous studies have shown that in both *Drosophila* embryos and cultured cells, Cid (the *Drosophila* homolog of the centromere protein CENP-A) depletion causes a block in prometaphase and a mitotic delay and that this phenotype is rescued by mutations (or RNAi) that abrogate the SAC (Blower *et al.* 2006; Pauleau *et al.* 2019). We therefore asked whether loss the CMG activity affects Cid recruitment at kinetochores. We made preparations from noncolchicine-treated larval brains of *Sld5*, *Psf3*, and *Mcm5* mutants and stained them for DNA, tubulin, and Cid. We examined late prophases and prometaphases of diploid cells and found that in mutant brains the number of Cid signals per cell is significantly reduced compared to control (Fig. 4). This finding agrees with the observation that mutant brains exhibit some diploid PMLES (Fig. 1b and e), which are a characteristic outcome of centromere/kinetochore defects (Somma *et al.* 2008; Renda *et al.* 2017; Pellacani *et al.* 2018; Pavlova *et al.* 2019). Collectively, our results suggest that loss of CMG activity causes incomplete DNA replication, DNA damage, and defective Cid recruitment at centromeres and that these conditions cooperate to trigger a strong SAC response that arrests the cells in prometaphase.

Previous studies in mammalian cells have shown that during the prolonged SAC-induced mitotic arrest there is a slow but continuous Cyclin B (Cyc B) degradation. When Cyc B falls below a critical threshold, mitotic cells undergo the "slippage" process and enter G1 without chromosome segregation (Brito and Rieder 2006; Brito *et al.* 2008). We thus assayed whether and to which extent diploid prometaphase cells of *Sld5*, *Psf3*, and *Mcm5* mutant brains retain Cyc B. Examination of preparations stained for Cyc

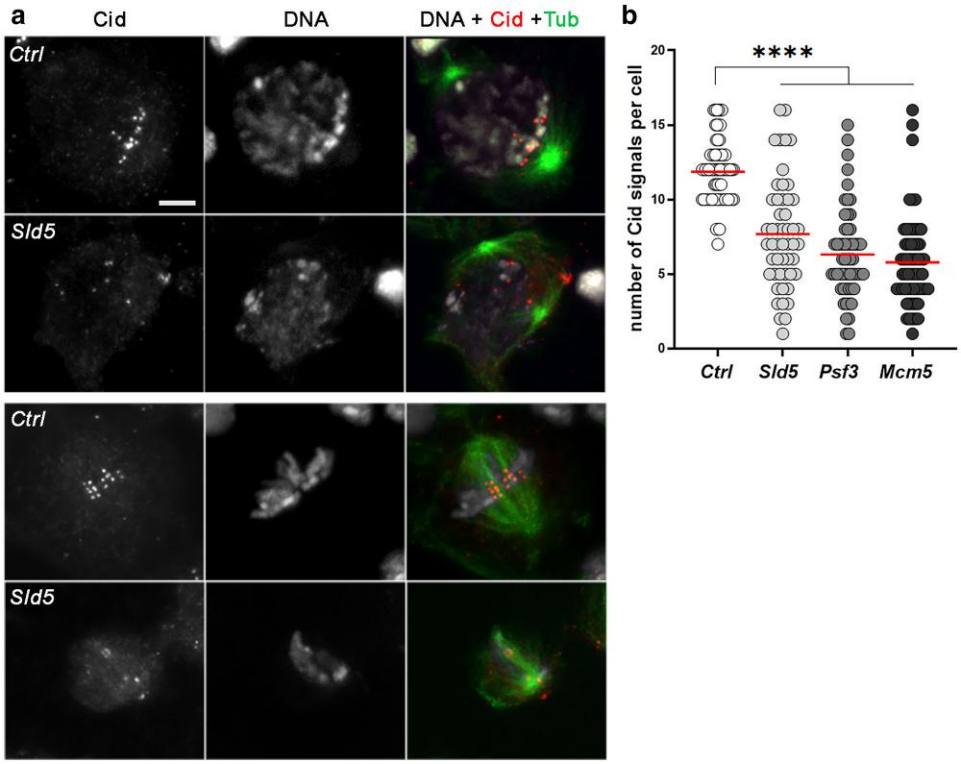

Fig. 4. Mutations in the CMG genes affect Cid recruitment at centromeres. a) Examples of diploid prophases (top panels) and metaphases/prometaphases (bottom panels) from control (*Ctrl*) and *Sld5* mutant brains stained for Cid (CENP-A), tubulin (Tub), and counterstained with DAPI. b) Scatter plots showing the distribution of mitotic cells (prophases, metaphases, and prometaphases) with different numbers of Cid signal in *Sld5*, *Psf3*, and *Mcm5* mutants. Scale bar, 5 μm. The plots and the statistical analysis were made using the GraphPad Prism Software 10.4.1. Significance was assessed by ANOVA and Tukey multiple comparison; $^{****}P < 0.0001$. The numbers of cells examined, in each case selected from 3 different brains, are as follows: Ctrl, 73; *Sld5*, 58; *Psf3*, 53; and *Mcm5*, 60.

B, tubulin, and DNA revealed that 98.8% prometaphase figures of control brains were strongly stained by anti-Cyc B antibodies. Most (90%) control metaphases were also stained for Cyc B, while virtually none of the anaphase and telophases were Cyc B-positive. In contrast, in *Sld5*, *Psf3*, and *Mcm5* mutant brains, the prometaphases strongly stained by anti-Cyc B antibodies were 44.4, 61.2, and 62.2%, respectively; the remaining prometaphases were either weakly stained or completely unstained. The few anaphases found in the mutants were all Cyc B-negative (Fig. 5; Supplementary Table 3). This result indicates that diploid mutant cells arrested in prometaphase are undergoing a gradual Cyc B decline that will eventually lead to their slippage to G1. Our data further suggest that many of these 4N G1 cells undergo an additional round of DNA replication giving rise to polyploid mitotic figures.

Mutations in *zw10* substantially modify the spindle phenotype of *Sld5* mutants

To further explore the SAC contribution to the mutant phenotype, we constructed males homozygous for *Sld5* and carrying a mutation in the X-linked *zw10* gene. *zw10* specifies an essential component of the SAC machinery [reviewed by Karess (2005)], and previous studies have shown that mutations in this gene release cells from the SAC-dependent mitotic block (Basto *et al.* 2000; Pellacani *et al.* 2018). The *zw10/FM7, Tb; Sld5/TM6B, Tb* females produced only a few double mutant male larvae that reached the early third instar. The brains of these larvae were very small and characterized by an extremely low MI, but showed frequencies of metaphases and anaphases significantly higher than those of *Sld5* homozygotes. In addition, they showed substantial reductions in the frequencies of unstructured spindles and polyploid cells compared with *Sld5* mutant males that were proficient for *zw10*. Finally, double mutant males displayed fewer and milder centrosome defects than *Sld5* homozygotes (Fig. 6; Supplementary Tables 4–6). A likely reason for the very low MI in *zw10; Sld5* double mutant brains is that the loss of the *zw10* function permits mutant cells with abnormally condensed and broken chromosomes to enter anaphase in a relatively early stage of brain development. This event would lead to daughter cells with highly unbalanced chromosome complements that would stop dividing or die. Thus, most of the dividing cells that we see in the double mutant are unlikely to be the descendants of cells that had suffered a prometaphase arrest. They would instead be cells produced by a relatively regular mitotic division, which divide again in the absence of SAC activity. These results support the hypothesis that a substantial fraction of the aberrant spindles observed in the *Sld5*, *Psf2*, *Psf3*, and *Mcm5* mutants represent different stages of spindle degeneration that follow the long SAC-dependent prometaphase arrest.

The centrosome defects observed in the CMG mutants are not the cause of the aberrant spindle morphology

As mentioned above, previous work on mammalian cells showed that the SLD5 protein localizes to the centrosomes and that its depletion affects centrosome integrity and duplication, leading to centrosome-dependent defects in spindle formation and morphology (Kaur *et al.* 2018). In the CMG mutants examined here, we

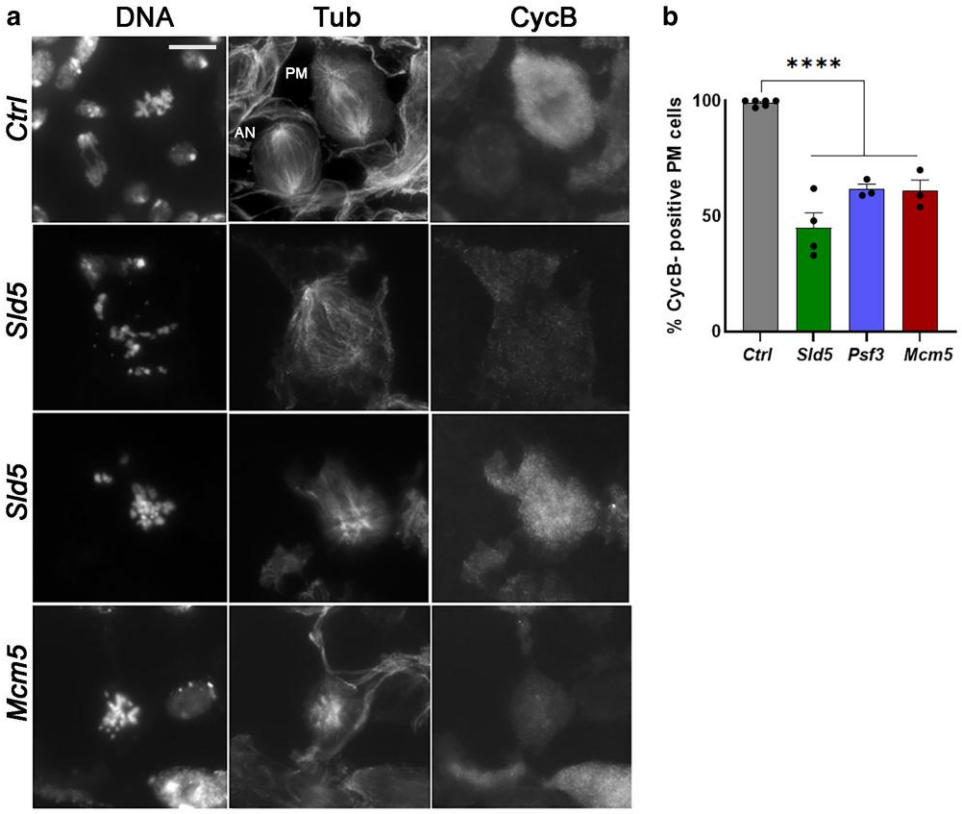

Fig. 5. Cyclin B behavior in control and CMG mutants. a) Examples of control and mutant cells immunostained for Cyclin B (Cyc B), tubulin (Tub), and counterstained with DAPI. The control panel shows a Cyc B-positive prometaphase (PM) and a Cyc B-negative anaphase (AN). The other panels show Cyc B-positive and negative PM-like cells observed in the indicated CMG mutants. Scale bar, 10 μm. b) Frequencies (±SEM) of Cyc B-positive PM-like cells in the CMG mutants. The dots represent frequencies observed in individual brains from 2 experiments. Significance was assessed by ANOVA and Tukey multiple comparison; ****$P < 0.0001$. See Supplementary Table 3 for detailed information about Cyc B localization in mitotic cells of the CMG mutants.

did not observe diploid cells with multipolar spindles, suggesting that centrosome fragmentation seen in these mutants does not give rise to this type of spindles (Figs. 1 and 3). In addition, the unstructured spindles without centrosomes observed in our mutants are unlikely to result from lack of centrosome activity. This conclusion is suggested by previous studies on mutants in genes that encode essential centrosomal components and lack functional centrosomes. The larval brain cells of these mutants form anastral but morphologically regular spindles that have full ability to mediate mitotic division and support development to the adulthood (Bonaccorsi *et al.* 2000; Megraw *et al.* 2001; Basto *et al.* 2006; Giansanti *et al.* 2008), reviewed by Gatti *et al.* (2012).

To provide support to this view, we generated *Psf3; Sas4* double mutants that are devoid of centrosomes due to lack of *Sas4* function (Basto *et al.* 2006). The larval brain cells of *Sas4* mutants, despite the absence of centrosomes, form morphologically regular and functional anastral spindles and survive to the adulthood (Basto *et al.* 2006). We confirmed that *Sas4* mutants exhibit anastral but otherwise regular spindles. We also found that *Psf3; Sas4* double mutant brains exhibit highly irregular spindles fully comparable to those seen in *Psf3* single mutants (Fig. 7; Supplementary Table 7). These results rule out the possibility that the aberrant spindles observed in *Psf3* mutants are generated by centrosomal abnormalities. They further suggest that in *Psf3* mutants, as well as in the other mutants in CMG genes, the spindle and centrosomal defects are largely independent consequences of a degeneration process caused by a prolonged SAC-mediated mitotic arrest.

Discussion

Inactivation of genes encoding different components of the CMG complex causes virtually identical phenotypes

We found that mutation in the CMG genes causes virtually identical phenotypes in *Drosophila* larval brains, consisting in severe defects in chromosome condensation, chromosome breakage, and the presence of numerous hyperploid/polyploid mitotic figures. Notably, mitotic phenotypes very similar to those described here have been observed in *Drosophila* mutants for different ORC genes (Loupart *et al.* 2000; Pflumm and Botchan 2001). This suggests that these phenotypes are the consequence of a common primary defect in DNA replication and do not reflect direct roles of these genes in the control of centrosome and spindle structure. Severely defective chromosome condensation and possibly chromosome breakage have been also found in human cells depleted of ORC2 by RNAi (Prasanth *et al.* 2004). While the chromosome breakage phenotype is easily attributable to defective DNA replication, the molecular mechanisms leading to aberrant chromosome condensation are currently unclear. Two possibilities have been considered. It has been proposed that DNA replication directly contributes to a longitudinal contraction of the chromosome and that a partial block in the replication machinery leads to aberrant condensation (Pflumm 2002). The other possibility is that defective DNA replication alters proper condensin recruitment to mitotic chromosomes (Prasanth *et al.* 2004). Our results do not allow discrimination between these 2 possibilities,

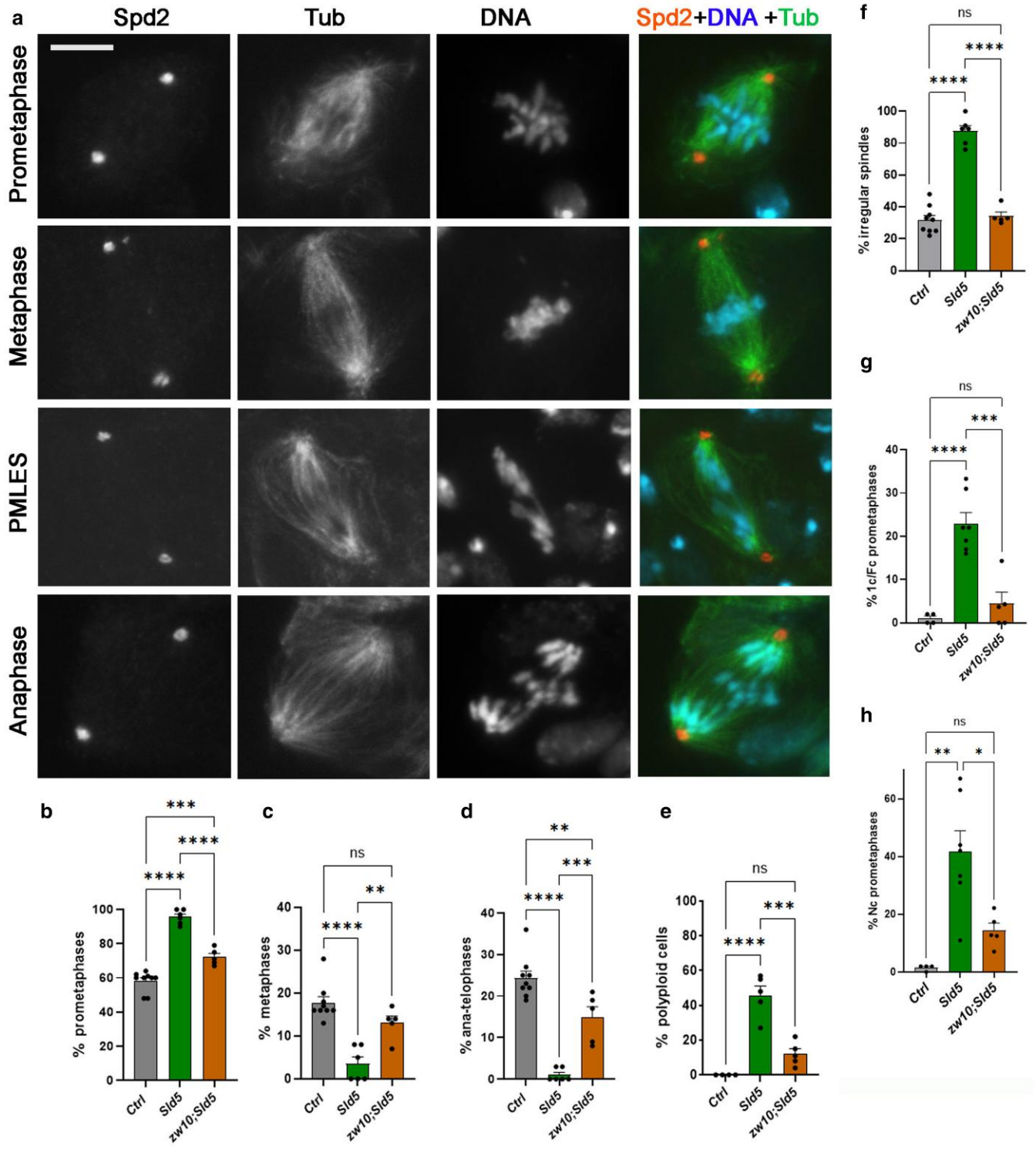

Fig. 6. Loss of the *zw10* function affects the mitotic behavior of *Sld5* mutant cells. a) Examples of dividing cells from *zw10*; *Sld5* double mutant brains. Note that these cells exhibit rather regular centrosomes and spindles. Scale bar, 10 μm. b–h) Comparison between controls, *Sld5* single mutants, and *zw10*; *Sld5* double mutants for the frequencies (±SEM) of diploid prometaphases, metaphases, and ana-telophases b–d), polyploid cells e), diploid cells with irregular spindles f), diploid cells with a single and/or fragmented centrosome g), or devoid of centrosomes h). For control (*Ctrl*) and *Sld5* single mutants, the dots represent frequencies observed in individual brains from 3 experiments. To characterize the double mutant, we performed 6 different experiments and scored 3–4 brains per experiment; each dot represents the average frequency per experiment. Significance was assessed by ANOVA and Tukey multiple comparison; ****, ***, and **: $P < 0.0001$, 0.001, and 0.01, respectively. See Supplementary Table 3 for a detailed account of the data used for the comparison.

which are not mutually exclusive. We only note that larval brains from mutants in different condensin-coding genes exhibit chromosome condensation phenotypes quite similar to those observed here in CMG mutants (Steffensen *et al.* 2001; Somma *et al.* 2003).

We also found that brains from CMG mutants exhibit defective Cid recruitment at centromeres. This finding is consistent with the hypothesis that DNA replication acts as an error correction mechanism to specifically maintain CENP-A at centromeres.

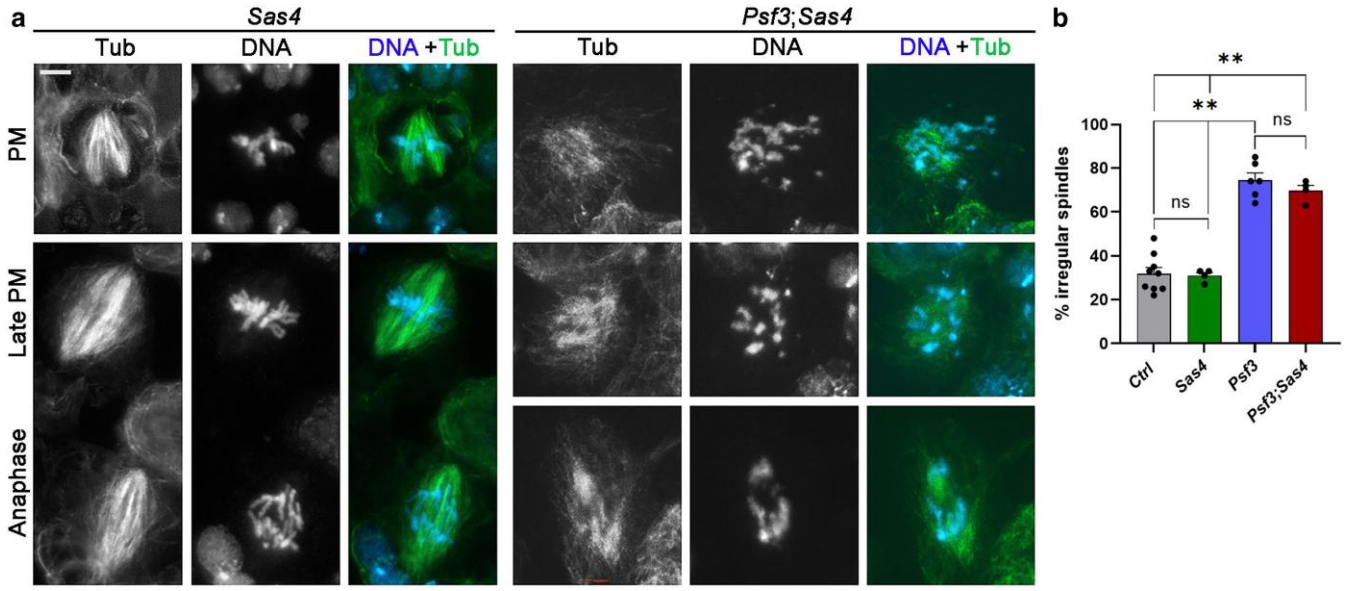

Fig. 7. Loss of *Sas4* does not improve the spindle defects caused by mutations in *Psf3*. a) Examples of spindles from *Sas4* single mutants and *Psf3*; *Sas4* double mutants. The early prometaphase (PM) of the *Sas4* single mutant exhibits a split spindle pole, while the late PM and the anaphase show anastral but otherwise morphologically regular spindles. In contrast, the spindles of the prometaphases from *Psf3*; *Sas4* double mutants are highly irregular. Scale bar, 5 μm. b) Frequencies of irregular spindles observed in control (*Ctrl*), *Sas4*, and *Psf3* mutants and in *Psf3*; *Sas4* double mutants. The dots represent frequencies observed in individual brains from at least 2 different experiments; error bar SEM. Significance was assessed by ANOVA and Tukey multiple comparison; $^{**}P < 0.01$. See Supplementary Table 4 for a detailed account of the data used for the comparison.

In human cells, during G1 CENP-A is associated with many sites on the chromosome arms. However, when cells pass through the S phase, the noncentromeric pool of CENP A is selectively removed, whereas centromeres retain CENP-A exploiting the activity of the CCAN complex (Constitutive Centromere Associated Network) (Nechemia-Arbely *et al.* 2019). Although our findings do not prove that the Cid phenotype observed in our mutants is a consequence of failures of a DNA replication-based error correction mechanism, they are fully compatible with this possibility.

The fact that knockout of *Psf2*, *Psf3*, or *Mcm5* results in virtually identical mitotic phenotypes and that these phenotypes are also very similar to those observed in mutants for different *Drosophila* ORC genes (Loupart *et al.* 2000; Pflumm and Botchan 2001) is consistent with the finding that mutations in the human orthologs of many of these genes cause the MGORS. Intriguingly, like the mutants in the *Drosophila* CMG and ORC genes that exhibit reduced larval brain growth, also MGORS is characterized by embryonic and postnatal growth retardation and microcephaly (Vetro *et al.* 2017; Ting *et al.* 2020; McQuaid *et al.* 2022; Nabais Sa *et al.* 2022).

Impaired CMG activity blocks entry into anaphase

We have shown that in the larval brains of *Sld5*, *Psf2*, *Psf3*, and *Mcm5* loss-of-function mutants, most dividing cells are in a prometaphase-like stage. In the same brains, the frequencies of metaphases with well-aligned chromosomes and the frequencies of anaphases were 3–7 times and 8–22 times lower than in controls, respectively (Fig. 1). Also in RNAi brains for these genes, as well as in *Psf1* and *Cdc45* RNAi brains, most dividing cells were in a prometaphase-like stage and the frequencies of metaphases and anaphases were significantly reduced compared to controls (Supplementary Fig. 4). These results indicate that the brain cells of mutants with compromised CMG activity and severely damaged chromosomes are strongly delayed in the prometaphase to anaphase transition. A block in anaphase entry following DNA damage and/or replication stress has been previously observed in different *Drosophila* tissues (Fogarty *et al.* 1997; Garner *et al.* 2001; Su and Jaklevic 2001; Laurencon *et al.* 2003; Royou *et al.* 2005), cultured human cells (Smits *et al.* 2000; Mikhailov and Rieder 2002; Novais-Cruz *et al.* 2023), *Caenorhabditis elegans* (Lawrence *et al.* 2015) and *Saccharomyces cerevisiae* (Kim and Burke 2008; Silva *et al.* 2014; Palou *et al.* 2017; Zhou *et al.* 2024). This block has been attributed to the DNA damage response (DDR) pathway (Fogarty *et al.* 1997; Smits *et al.* 2000; Laurencon *et al.* 2003), or the SAC pathway (Mikhailov and Rieder 2002), or more often to both pathways (Royou *et al.* 2005; Kim and Burke 2008; Silva *et al.* 2014; Lawrence *et al.* 2015; Palou *et al.* 2017; Novais-Cruz *et al.* 2023; Zhou *et al.* 2024). Cumulative evidence indicates that the DDR and SAC proteins interact to trigger the SAC response and prevent the anaphase onset [reviewed by Luna-Maldonado *et al.* (2021)]. Of particular interest in this context are studies on *Drosophila* larval brains showing that the block in anaphase entry caused by extensive X-irradiation is partially rescued by mutations in either *grp/Chk1* or *bubR1* that inactivate the DDR and SAC pathway, respectively (Royou *et al.* 2005).

Our phenotypic analyses strongly suggest that the multiple CABs and the incompletely replicated DNA resulting from the compromised CMG function trigger the DDR, which would in turn trigger the SAC. In addition, it is quite likely that the defective Cid recruitment at the centromeres of mutant chromosomes (Fig. 4) affects kinetochore assembly, generating the SAC response as previously observed in both embryonic and cultured *Drosophila* cells (Blower *et al.* 2006; Pauleau *et al.* 2019). Consistent with a SAC-mediated mitotic block, in *Sld5*, *Psf3*, and *Mcm5* mutant brains, there were many (45–62%) prometaphase-like cells with low Cyc B contents and high frequencies of polyploid cells. In contrast, in control brains, nearly all (99%) prometaphases had strong Cyclin B signals and polyploid mitoses were virtually absent. Similar observations were made on a variety of mammalian cells arrested in a prometaphase-like stage by the SAC activity. It has been proposed that the SAC-arrested cells undergo mitotic

slippage, consisting in a gradual degradation of Cyc B that eventually leads to mitosis exit and return to interphase; once in interphase, the cells can either die or replicate their DNA and become polyploid (Brito and Rieder 2006; Sloss et al. 2016).

The hypothesis that also in our mutants the SAC activity is the main cause of the delayed transition from a prometaphase-like stage to anaphase is strongly supported by the analysis of *zw10*; *Sld5* double mutants, in which the SAC function is compromised by loss of the *zw10* activity. Indeed, in the brains of these mutants, the frequency of anaphases is significantly higher than in those of *Sld5* single mutants, while the frequency of polyploid figures is lower. Moreover, *zw10*; *Sld5* double mutants showed fewer spindle and centrosome aberrations compared with *Sld5* mutants that were proficient for *zw10*. These results support the hypothesis that many of these spindle and centrosome defects observed in the *Sld5* single mutant represent different stages of spindle degeneration that follow the SAC-dependent prometaphase arrest. In line with this interpretation, the few metaphases and anaphases/telophases observed in CMG mutant and RNAi brains mostly exhibit regular bipolar spindles, indicating that cells that manage to escape the SAC and enter anaphase do not usually exhibit spindle disorganization.

Impaired CMG activity leads to centrosome and spindle defects

We have shown that mutations in the CMG genes cause a variety of centrosome defects, including centrosome fragmentation, the presence of a single and often large centrosome in both diploid and polyploid cells, and the complete absence of centrosomes. Strong effects of DNA damage and/or replication stress on centrosomes have been previously observed in different systems. Early studies on *Drosophila* embryos showed that mutations in genes involved in the DDR pathway, treatments with the DNA replication inhibitor aphidicolin and a variety of DNA damaging agents, all lead to dissociation of γ-tubulin ring components from mitotic centrosomes and concomitant defects in spindle structure and chromosome segregation (Sibon et al. 2000; Takada et al. 2003). Studies on mammalian cells showed that hydroxyurea-induced DNA replication stress and DNA damage lead to the formation of supernumerary centrosomes and spindle defects (Meraldi et al. 1999; Hut et al. 2003). Similar results were obtained with chicken DT40 cells bearing DNA damage induced by loss of Rad51 or by the combined action of ionizing radiation and Rad54 deficiency. These cells, following a prolonged G2 arrest, formed supernumerary centrosomes that resulted in multipolar spindles (Dodson et al. 2004). More recent work has shown that the initial event that leads to centrosome amplification in cells with damaged or incompletely replicated DNA, and/or arrested in prometaphase by SAC activity, is premature centriole disengagement. In normal cells, centriole disengagement is mediated by separase and polo-like kinase 1 (PLK1) and normally occurs at mitotic exit, licensing centrosome duplication (Tsou et al. 2009). Human cells (hTERT-RPE1) exposed to mild aphidicolin-induced replication stress showed premature centriole disengagement in G2, mediated by the ATR-Chk1 axis of the DDR (Wilhelm et al. 2019; Dwivedi et al. 2023). Similarly, RPE1 cells arrested in prometaphase by monastrol treatment and SAC activity displayed centriole disengagement and centrosome fragmentation (Karki et al. 2017). Interestingly, analysis of live cells showed that the separated centrosome fragments often reassociate within 25 min of monastrol washout, a dynamic behavior that might explain why we observe a variety of centrosome phenotypes in fixed larval brain cells of CMG mutants.

Previous work on mammalian cells showed that many proteins involved in DNA replication localize to the centrosomes and affect centrosome structure and/or behavior [reviewed by Knockleby and Lee (2010)]. Notably, depletion of some of these proteins mimicked the phenotype observed in the CMG mutants examined here. For example, it has been shown that in HeLa cells, SLD5 localizes to the centrosomes and that its RNAi-mediated depletion causes mitotic phenotypes quite similar to those we observed in *Drosophila* GINS mutants, namely, defective chromosome condensation, abnormal PCM recruitment and centrosome fragmentation, arrest in a prometaphase-like stage with uncongressed chromosomes, and morphologically abnormal and multipolar spindles (Kaur et al. 2018). The same phenotypes were also observed in HeLa cells depleted of ORC2, which also localizes to the centrosomes (Prasanth et al. 2004). These phenotypes, although not always together, have been also observed in human cells depleted of other DNA replication proteins that localize to the centrosomes [reviewed by Knockleby and Lee (2010)]. Although the precise mechanisms leading to irregular spindle morphology after depletion of these proteins are currently unclear, it has been generally proposed that the spindle defects are at least in part the consequence of aberrant MT nucleation caused by centrosome fragmentation/amplification (Prasanth et al. 2004; Hemerly et al. 2009; Knockleby and Lee 2010; Kaur et al. 2018).

In-depth studies on the possible localization of CMG proteins at the *Drosophila* centrosomes have never been performed. However, immunolocalization experiments suggest that Cdc45 does not accumulate in the centrosomes (Loebel et al. 2000). In addition, proteomic analyses of isolated centrosomes from *Drosophila* embryos identified 251 proteins that included both Orc1 and Orc2 but none of the components of the CMG complex (Muller et al. 2010). It is therefore conceivable that, in contrast to mammalian cells, *Drosophila* centrosomes do not accumulate CMG proteins. Regardless a possible enrichment of CMG proteins in the centrosomes, our data strongly suggest that the mitotic phenotype observed in the mutants is not a consequence of a primary centrosome defect, but rather the result of progressive degeneration processes affecting spindles and centrosomes, following a prolonged SAC-mediated mitotic arrest. This hypothesis is supported by several findings. The centrosome phenotype observed in mutant brains is rather different from those observed in human cells subjected to replication stress and/or DNA damage or depleted of DNA replication proteins that localize to the centrosomes. We see cells with fragmented centrosomes, cells containing a single and often large centrosome, and, above all, cells without detectable centrosomes. We believe that these phenotypes reflect a degeneration process that starts with centrosome fragmentation, progresses though various degrees of reaggregation of the fragments as observed in mammalian cells (Karki et al. 2017), and ends up with the complete disappearance of centrosomes. The centrosome fragmentation observed in the mutants is unlikely to affect the spindle structure, as most of the fragments do not appear to have MT nucleating ability and do not give rise to multipolar spindles. In addition, most of the single large centrosomes observed in both diploid and polyploid cells have little or no MT nucleating abilities. Most importantly, we found that *Psf3; Sas4* double mutant brains that lack the centrosomes have the same spindle defects as *Psf3* singly mutant brains. Thus, it appears that mutant cells arrested in prometaphase by the SAC undergo independent processes of centrosome and spindle degeneration.

In summary, to explain our observations, we propose the following model (Fig. 8). After the replication stress caused by

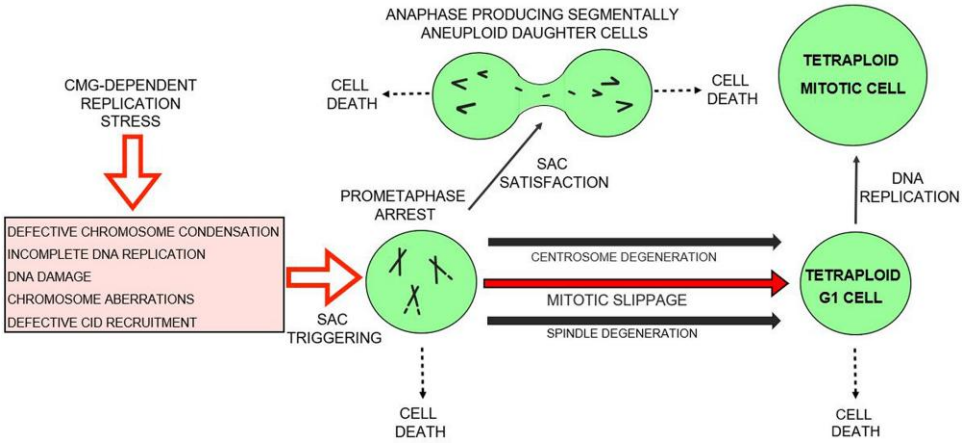

Fig. 8. A model for the cellular consequences of the CMG-dependent replication stress. Loss of the CMG activity causes a strong replication stress resulting in incompletely replicated and damaged DNA, defects in chromosome condensation and integrity, and reduced Cid recruitment at centromeres. These defects trigger the SAC that arrests the cells in prometaphase. Continuous lines indicate the outcomes of this arrest suggested by our data; the dotted lines indicate outcomes suggested by the literature [see for example Cheng and Crasta (2017)]. Some of the arrested cells will die, while others will be subjected to 2 fates. A small number of arrested cells would satisfy the SAC and enter anaphase. However, due to the abnormal chromosome condensation and extensive breakage, many of these anaphases will generate daughter cells with segmental aneuploidies that will probably lead to cell death. Most arrested prometaphases would instead undergo Cyclin B degradation, "slip" to interphase, and either die or replicate their DNA, giving rise to polyploid mitoses. During the prometaphase arrest, cells undergo independent processes of spindle and centrosome degeneration, which will eventually lead to unstructured spindles and to the disruption of centrosome organization.

loss-of-function mutations in the CMG genes, cells enter mitosis with incompletely replicated DNA, severe defects in chromosome condensation, extensive chromosome breakage, and reduced Cid incorporation at centromeres. All these conditions trigger the SAC that arrests the cells in a prometaphase-like stage. Some of the arrested prometaphases would manage to align the chromosomes, satisfy the SAC, and enter anaphase. However, many of these anaphases would generate daughter cells with segmental aneuploidies that will probably die. Most arrested prometaphases would instead undergo a progressive degradation of Cyc B, and when Cyc B falls below a critical threshold, the cells would return to interphase, replicate their DNA, and become polyploid. During their prolonged stay in prometaphase, cells undergo independent and probably progressive processes of spindle and centrosome degradation that eventually lead to completely unstructured spindles and the absence of detectable centrosomes. We were able to propose this model because we made our observations on *Drosophila* larval brains in which the cells arrested in prometaphase can survive for a relatively long time in a natural context. Thus, our model might also apply to vertebrate cells, and more specifically to human cancer cells, growing in the same conditions as those of *Drosophila* brains.

Data availability

The authors affirm that all data necessary for confirming the conclusions of the article are present within the article, figures, tables, and supplementary materials.

Supplemental material available at GENETICS online.

Acknowledgments

We thank Gary Karpen and Christian Lehner for generously providing us with the anti-Cid and anti-Cyc B antibodies and Maria Patrizia Somma for the critical reading of the manuscript and helpful suggestions. We also thank the Bloomington and Kyoto Stock Centers and the Vienna Drosophila Resource Center for the fly stocks.

Funding

This work was supported by grants from the AIRC Foundation for Cancer Research to M.G. (AIRC IG16020) and G.D.R. (AIRC IG 26496).

Conflicts of interest

The authors declare no conflicts of interest.

Literature cited

Andreyeva EN, Kolesnikova TD, Belyaeva ES, Glaser RL, Zhimulev IF. 2008. Local DNA underreplication correlates with accumulation of phosphorylated H2Av in the Drosophila melanogaster polytene chromosomes. Chromosome Res. 16(6):851–862. doi:10.1007/s10577-008-1244-4.

Attali I, Botchan MR, Berger JM. 2021. Structural mechanisms for replicating DNA in eukaryotes. Annu Rev Biochem. 90(1):77–106. doi:10.1146/annurev-biochem-090120-125407.

Baker BS, Smith DA, Gatti M. 1982. Region-specific effects on chromosome integrity of mutations at essential loci in Drosophila melanogaster. Proc Natl Acad Sci U S A. 79(4):1205–1209. doi:10.1073/pnas.79.4.1205.

Basto R, Gomes R, Karess RE. 2000. Rough deal and Zw10 are required for the metaphase checkpoint in Drosophila. Nat Cell Biol. 2(12):939–943. doi:10.1038/35046592.

Basto R, Lau J, Vinogradova T, Gardiol A, Woods CG, Khodjakov A, Raff JW. 2006. Flies without centrioles. Cell. 125(7):1375–1386. doi:10.1016/j.cell.2006.05.025.

Bernard F, Picard C, Cormier-Daire V, Eidenschenk C, Pinto G, Bustamante JC, Jouanguy E, Teillac-Hamel D, Colomb V, Funck-Brentano I, *et al.* 2004. A novel developmental and immunodeficiency syndrome associated with intrauterine growth retardation and a lack of natural killer cells. Pediatrics. 113(1):136–141. doi:10.1542/peds.113.1.136.

Bicknell LS, Bongers EM, Leitch A, Brown S, Schoots J, Harley ME, Aftimos S, Al-Aama JY, Bober M, Brown PA, *et al.* 2011.

Mutations in the pre-replication complex cause Meier-Gorlin syndrome. Nat Genet. 43(4):356–359. doi:10.1038/ng.775.

Blower MD, Daigle T, Kaufman T, Karpen GH. 2006. Drosophila CENP-A mutations cause a BubR1-dependent early mitotic delay without normal localization of kinetochore components. PLoS Genet. 2(7):e110. doi:10.1371/journal.pgen.0020110.

Blower MD, Karpen GH. 2001. The role of Drosophila CID in kinetochore formation, cell-cycle progression and heterochromatin interactions. Nat Cell Biol. 3(8):730–739. doi:10.1038/35087045.

Bonaccorsi S, Giansanti MG, Gatti M. 2000. Spindle assembly in Drosophila neuroblasts and ganglion mother cells. Nat Cell Biol. 2(1):54–56. doi:10.1038/71378.

Brito DA, Rieder CL. 2006. Mitotic checkpoint slippage in humans occurs via cyclin B destruction in the presence of an active checkpoint. Curr Biol. 16(12):1194–1200. doi:10.1016/j.cub.2006.04.043.

Brito DA, Yang Z, Rieder CL. 2008. Microtubules do not promote mitotic slippage when the spindle assembly checkpoint cannot be satisfied. J Cell Biol. 182(4):623–629. doi:10.1083/jcb.200805072.

Cenci G, Rawson RB, Belloni G, Castrillon DH, Tudor M, Petrucci R, Goldberg ML, Wasserman SA, Gatti M. 1997. Ubcd1, a Drosophila ubiquitin-conjugating enzyme required for proper telomere behavior. Genes Dev. 11(7):863–875. doi:10.1101/gad.11.7.863.

Cenci G, Siriaco G, Raffa GD, Kellum R, Gatti M. 2003. The Drosophila HOAP protein is required for telomere capping. Nat Cell Biol. 5(1):82–84. doi:10.1038/ncb902.

Cheng B, Crasta K. 2017. Consequences of mitotic slippage for antimicrotubule drug therapy. Endocr Relat Cancer. 24(9):T97–T106. doi:10.1530/ERC-17-0147.

Chmielewski JP, Henderson L, Smith CM, Christensen TW. 2012. Drosophila Psf2 has a role in chromosome condensation. Chromosoma. 121(6):585–596. doi:10.1007/s00412-012-0383-8.

Christensen TW, Tye BK. 2003. Drosophila MCM10 interacts with members of the prereplication complex and is required for proper chromosome condensation. Mol Biol Cell. 14(6):2206–2215. doi:10.1091/mbc.e02-11-0706.

Conduit PT, Richens JH, Wainman A, Holder J, Vicente CC, Pratt MB, Dix CI, Novak ZA, Dobbie IM, Schermelleh L, et al. 2014. A molecular mechanism of mitotic centrosome assembly in Drosophila. Elife. 3:e03399. doi:10.7554/eLife.03399.

Crevel G, Hashimoto R, Vass S, Sherkow J, Yamaguchi M, Heck MM, Cotterill S. 2007. Differential requirements for MCM proteins in DNA replication in Drosophila S2 cells. PLoS One. 2(9):e833. doi:10.1371/journal.pone.0000833.

Dodson H, Bourke E, Jeffers LJ, Vagnarelli P, Sonoda E, Takeda S, Earnshaw WC, Merdes A, Morrison C. 2004. Centrosome amplification induced by DNA damage occurs during a prolonged G2 phase and involves ATM. EMBO J. 23(19):3864–3873. doi:10.1038/sj.emboj.7600393.

Dwivedi D, Harry D, Meraldi P. 2023. Mild replication stress causes premature centriole disengagement via a sub-critical Plk1 activity under the control of ATR-Chk1. Nat Commun. 14(1):6088. doi:10.1038/s41467-023-41753-1.

Ferguson RL, Maller JL. 2008. Cyclin E-dependent localization of MCM5 regulates centrosome duplication. J Cell Sci. 121(19):3224–3232. doi:10.1242/jcs.034702.

Fogarty P, Campbell SD, Abu-Shumays R, Phalle BS, Yu KR, Uy GL, Goldberg ML, Sullivan W. 1997. The Drosophila grapes gene is related to checkpoint gene chk1/rad27 and is required for late syncytial division fidelity. Curr Biol. 7(6):418–426. doi:10.1016/S0960-9822(06)00189-8.

Fragkos M, Choleza M, Papadopoulou P. 2023. The role of gammaH2AX in replication stress-induced carcinogenesis: possible links and recent developments. Cancer Diagn Progn. 3(6):639–648. doi:10.21873/cdp.10266.

Gambus A, Jones RC, Sanchez-Diaz A, Kanemaki M, van Deursen F, Edmondson RD, Labib K. 2006. GINS maintains association of Cdc45 with MCM in replisome progression complexes at eukaryotic DNA replication forks. Nat Cell Biol. 8(4):358–366. doi:10.1038/ncb1382.

Garner M, van Kreeveld S, Su TT. 2001. mei-41 and bub1 block mitosis at two distinct steps in response to incomplete DNA replication in Drosophila embryos. Curr Biol. 11(20):1595–1599. doi:10.1016/S0960-9822(01)00483-3.

Gatti M. 1979. Genetic control of chromosome breakage and rejoining in Drosophila melanogaster: spontaneous chromosome aberrations in X-linked mutants defective in DNA metabolism. Proc Natl Acad Sci U S A. 76(3):1377–1381. doi:10.1073/pnas.76.3.1377.

Gatti M, Baker BS. 1989. Genes controlling essential cell-cycle functions in Drosophila melanogaster. Genes Dev. 3(4):438–453. doi:10.1101/gad.3.4.438.

Gatti M, Bucciarelli E, Lattao R, Pellacani C, Mottier-Pavie V, Giansanti MG, Somma MP, Bonaccorsi S. 2012. The relative roles of centrosomal and kinetochore-driven microtubules in Drosophila spindle formation. Exp Cell Res. 318(12):1375–1380. doi:10.1016/j.yexcr.2012.05.001.

Gatti M, Tanzarella C, Olivieri G. 1974. Analysis of the chromosome aberrations induced by x-rays in somatic cells of Drosophila melanogaster. Genetics. 77(4):701–719. doi:10.1093/genetics/77.4.701.

Giansanti MG, Bucciarelli E, Bonaccorsi S, Gatti M. 2008. Drosophila SPD-2 is an essential centriole component required for PCM recruitment and astral-microtubule nucleation. Curr Biol. 18(4):303–309. doi:10.1016/j.cub.2008.01.058.

Gouge CA, Christensen TW. 2010. Drosophila Sld5 is essential for normal cell cycle progression and maintenance of genomic integrity. Biochem Biophys Res Commun. 400(1):145–150. doi:10.1016/j.bbrc.2010.08.033.

Hemerly AS, Prasanth SG, Siddiqui K, Stillman B. 2009. Orc1 controls centriole and centrosome copy number in human cells. Science. 323(5915):789–793. doi:10.1126/science.1166745.

Homem CC, Knoblich JA. 2012. Drosophila neuroblasts: a model for stem cell biology. Development. 139(23):4297–4310. doi:10.1242/dev.080515.

Hut HM, Lemstra W, Blaauw EH, Van Cappellen GW, Kampinga HH, Sibon OC. 2003. Centrosomes split in the presence of impaired DNA integrity during mitosis. Mol Biol Cell. 14(5):1993–2004. doi:10.1091/mbc.e02-08-0510.

Ilves I, Petojevic T, Pesavento JJ, Botchan MR. 2010. Activation of the MCM2-7 helicase by association with Cdc45 and GINS proteins. Mol Cell. 37(2):247–258. doi:10.1016/j.molcel.2009.12.030.

Karess R. 2005. Rod-Zw10-Zwilch: a key player in the spindle checkpoint. Trends Cell Biol. 15(7):386–392. doi:10.1016/j.tcb.2005.05.003.

Karki M, Keyhaninejad N, Shuster CB. 2017. Precocious centriole disengagement and centrosome fragmentation induced by mitotic delay. Nat Commun. 8(1):15803. doi:10.1038/ncomms15803.

Kaur M, Devi R, Ghosh T, Khan MM, Kumar P, Priyanka KA, Sharma A, Varshney A, Kumar V, Saxena S. 2018. Sld5 ensures centrosomal resistance to congression forces by preserving centriolar satellites. Mol Cell Biol. 38(2):e00371-17. doi:10.1128/MCB.00371-17.

Kim EM, Burke DJ. 2008. DNA damage activates the SAC in an ATM/ATR-dependent manner, independently of the kinetochore. PLoS Genet. 4(2):e1000015. doi:10.1371/journal.pgen.1000015.

Knapp KM, Jenkins DE, Sullivan R, Harms FL, von Elsner L, Ockeloen CW, de Munnik S, Bongers EMHF, Murray J, Pachter N, et al. 2021. MCM complex members MCM3 and MCM7 are associated with a phenotypic spectrum from Meier-Gorlin syndrome to

lipodystrophy and adrenal insufficiency. Eur J Hum Genet. 29(7): 1110–1120. doi:10.1038/s41431-021-00839-4.
Knockleby J, Lee H. 2010. Same partners, different dance: involvement of DNA replication proteins in centrosome regulation. Cell Cycle. 9(22):4487–4491. doi:10.4161/cc.9.22.14047.
Lattao R, Bonaccorsi S, Guan X, Wasserman SA, Gatti M. 2011. Tubby-tagged balancers for the Drosophila X and second chromosomes. Fly (Austin). 5(4):369–370. doi:10.4161/fly.5.4.17283.
Laurencon A, Purdy A, Sekelsky J, Hawley RS, Su TT. 2003. Phenotypic analysis of separation-of-function alleles of MEI-41, Drosophila ATM/ATR. Genetics. 164(2):589–601. doi:10.1093/genetics/164.2.589.
Lawrence KS, Chau T, Engebrecht J. 2015. DNA damage response and spindle assembly checkpoint function throughout the cell cycle to ensure genomic integrity. PLoS Genet. 11(4):e1005150. doi:10.1371/journal.pgen.1005150.
Lehner CF, O'Farrell PH. 1990. The roles of Drosophila cyclins A and B in mitotic control. Cell. 61(3):535–547. doi:10.1016/0092-8674(90)90535-M.
Loebel D, Huikeshoven H, Cotterill S. 2000. Localisation of the DmCdc45 DNA replication factor in the mitotic cycle and during chorion gene amplification. Nucleic Acids Res. 28(20):3897–3903. doi:10.1093/nar/28.20.3897.
Loupart ML, Krause SA, Heck MS. 2000. Aberrant replication timing induces defective chromosome condensation in Drosophila ORC2 mutants. Curr Biol. 10(24):1547–1556. doi:10.1016/S0960-9822(00)00844-7.
Luna-Maldonado F, Andonegui-Elguera MA, Diaz-Chavez J, Herrera LA. 2021. Mitotic and DNA damage response proteins: maintaining the genome stability and working for the common good. Front Cell Dev Biol. 9:700162. doi:10.3389/fcell.2021.700162.
Martinez MP, Wacker AL, Bruck I, Kaplan DL. 2017. Eukaryotic replicative helicase subunit interaction with DNA and its role in DNA replication. Genes (Basel). 8(4):117. doi:10.3390/genes8040117.
McQuaid ME, Ahmed K, Tran S, Rousseau J, Shaheen R, Kernohan KD, Yuki KE, Grover P, Dreseris ES, Ahmed S, *et al.* 2022. Hypomorphic GINS3 variants alter DNA replication and cause Meier-Gorlin syndrome. JCI Insight. 7(10):e155648. doi:10.1172/jci.insight.155648.
Megraw TL, Kao LR, Kaufman TC. 2001. Zygotic development without functional mitotic centrosomes. Curr Biol. 11(2):116–120. doi:10.1016/S0960-9822(01)00017-3.
Meraldi P, Lukas J, Fry AM, Bartek J, Nigg EA. 1999. Centrosome duplication in mammalian somatic cells requires E2F and Cdk2-cyclin A. Nat Cell Biol. 1(2):88–93. doi:10.1038/10054.
Mikhailov A, Rieder CL. 2002. Cell cycle: stressed out of mitosis. Curr Biol. 12(9):R331–R333. doi:10.1016/S0960-9822(02)00833-3.
Mitchell C, Becker V, DeLoach J, Nestore E, Bolterstein E, Kohl KP. 2022. The Drosophila Mutagen-Sensitivity Gene mus109 Encodes DmDNA2. Genes (Basel). 13(2):312. doi:10.3390/genes13020312.
Moyer SE, Lewis PW, Botchan MR. 2006. Isolation of the Cdc45/Mcm2-7/GINS (CMG) complex, a candidate for the eukaryotic DNA replication fork helicase. Proc Natl Acad Sci U S A. 103(27):10236–10241. doi:10.1073/pnas.0602400103.
Müller H, Schmidt D, Steinbrink S, Mirgorodskaya E, Lehmann V, Habermann K, Dreher F, Gustavsson N, Kessler T, Lehrach H, *et al.* 2010. Proteomic and functional analysis of the mitotic Drosophila centrosome. EMBO J. 29(19):3344–3357. doi:10.1038/emboj.2010.210.
Nabais Sá MJ, Miller KA, McQuaid M, Koelling N, Wilkie AOM, Wurtele H, de Brouwer APM, Oliveira J. 2022. Biallelic GINS2 variant p.(Arg114Leu) causes Meier-Gorlin syndrome with craniosynostosis. J Med Genet. 59(8):776–780. doi:10.1136/jmedgenet-2020-107572.
Nechemia-Arbely Y, Miga KH, Shoshani O, Aslanian A, McMahon MA, Lee AY, Fachinetti D, Yates JR 3rd, Ren B, Cleveland DW. 2019. DNA replication acts as an error correction mechanism to maintain centromere identity by restricting CENP-A to centromeres. Nat Cell Biol. 21(6):743–754. doi:10.1038/s41556-019-0331-4.
Novais-Cruz M, Pombinho A, Sousa M, Maia AF, Maiato H, Ferrás C. 2023. Mitotic DNA damage promotes chromokinesin-mediated missegregation of polar chromosomes in cancer cells. Mol Biol Cell. 34(5):ar47. doi:10.1091/mbc.E22-11-0518.
Pacek M, Tutter AV, Kubota Y, Takisawa H, Walter JC. 2006. Localization of MCM2-7, Cdc45, and GINS to the site of DNA unwinding during eukaryotic DNA replication. Mol Cell. 21(4): 581–587. doi:10.1016/j.molcel.2006.01.030.
Palou R, Palou G, Quintana DG. 2017. A role for the spindle assembly checkpoint in the DNA damage response. Curr Genet. 63(2): 275–280. doi:10.1007/s00294-016-0634-y.
Parker MW, Botchan MR, Berger JM. 2017. Mechanisms and regulation of DNA replication initiation in eukaryotes. Crit Rev Biochem Mol Biol. 52(2):107–144. doi:10.1080/10409238.2016.1274717.
Pauleau AL, Bergner A, Kajtez J, Erhardt S. 2019. The checkpoint protein Zw10 connects CAL1-dependent CENP-A centromeric loading and mitosis duration in Drosophila cells. PLoS Genet. 15(9): e1008380. doi:10.1371/journal.pgen.1008380.
Pavlova GA, Popova JV, Andreyeva EN, Yarinich LA, Lebedev MO, Razuvaeva AV, Dubatolova TD, Oshchepkova AL, Pellacani C, Somma MP, *et al.* 2019. RNAi-mediated depletion of the NSL complex subunits leads to abnormal chromosome segregation and defective centrosome duplication in Drosophila mitosis. PLoS Genet. 15(9):e1008371. doi:10.1371/journal.pgen.1008371.
Pellacani C, Bucciarelli E, Renda F, Hayward D, Palena A, Chen J, Bonaccorsi S, Wakefield JG, Gatti M, Somma MP. 2018. Splicing factors Sf3A2 and Prp31 have direct roles in mitotic chromosome segregation. Elife. 7:e40325. doi:10.7554/eLife.40325.
Pflumm MF. 2002. The role of DNA replication in chromosome condensation. Bioessays. 24(5):411–418. doi:10.1002/bies.10092.
Pflumm MF, Botchan MR. 2001. Orc mutants arrest in metaphase with abnormally condensed chromosomes. Development. 128(9):1697–1707. doi:10.1242/dev.128.9.1697.
Prasanth SG, Prasanth KV, Siddiqui K, Spector DL, Stillman B. 2004. Human Orc2 localizes to centrosomes, centromeres and heterochromatin during chromosome inheritance. EMBO J. 23(13): 2651–2663. doi:10.1038/sj.emboj.7600255.
Renda F, Pellacani C, Strunov A, Bucciarelli E, Naim V, Bosso G, Kiseleva E, Bonaccorsi S, Sharp DJ, Khodjakov A, *et al.* 2017. The Drosophila orthologue of the INT6 onco-protein regulates mitotic microtubule growth and kinetochore structure. PLoS Genet. 13(5): e1006784. doi:10.1371/journal.pgen.1006784.
Royou A, Macias H, Sullivan W. 2005. The Drosophila Grp/Chk1 DNA damage checkpoint controls entry into anaphase. Curr Biol. 15(4): 334–339. doi:10.1016/j.cub.2005.02.026.
Sekelsky J. 2017. DNA repair in Drosophila: mutagens, models, and missing genes. Genetics. 205(2):471–490. doi:10.1534/genetics.116.186759.
Sibon OC, Kelkar A, Lemstra W, Theurkauf WE. 2000. DNA-replication/DNA-damage-dependent centrosome inactivation in Drosophila embryos. Nat Cell Biol. 2(2):90–95. doi:10.1038/35000041.
Silva BA, Stambaugh JR, Yokomori K, Shah JV, Berns MW. 2014. DNA damage to a single chromosome end delays anaphase onset. J Biol Chem. 289(33):22771–22784. doi:10.1074/jbc.M113.535955.

Sloss O, Topham C, Diez M, Taylor S. 2016. Mcl-1 dynamics influence mitotic slippage and death in mitosis. Oncotarget. 7(5): 5176–5192. doi:10.18632/oncotarget.6894.

Smits VA, Klompmaker R, Arnaud L, Rijksen G, Nigg EA, Medema RH. 2000. Polo-like kinase-1 is a target of the DNA damage checkpoint. Nat Cell Biol. 2(9):672–676. doi:10.1038/35023629.

Somma MP, Ceprani F, Bucciarelli E, Naim V, De Arcangelis V, Piergentili R, Palena A, Ciapponi L, Giansanti MG, Pellacani C, *et al.* 2008. Identification of Drosophila mitotic genes by combining co-expression analysis and RNA interference. PLoS Genet. 4(7):e1000126. doi:10.1371/journal.pgen.1000126.

Somma MP, Fasulo B, Siriaco G, Cenci G. 2003. Chromosome condensation defects in barren RNA-interfered Drosophila cells. Genetics. 165(3):1607–1611. doi:10.1093/genetics/165.3.1607.

Steffensen S, Coelho PA, Cobbe N, Vass S, Costa M, Hassan B, Prokopenko SN, Bellen H, Heck MM, Sunkel CE. 2001. A role for Drosophila SMC4 in the resolution of sister chromatids in mitosis. Curr Biol. 11(5):295–307. doi:10.1016/S0960-9822(01)00096-3.

Su TT. 2011. Safeguarding genetic information in Drosophila. Chromosoma. 120(6):547–555. doi:10.1007/s00412-011-0342-9.

Su TT, Jaklevic B. 2001. DNA damage leads to a Cyclin A-dependent delay in metaphase-anaphase transition in the Drosophila gastrula. Curr Biol. 11(1):8–17. doi:10.1016/S0960-9822(00)00042-7.

Takada S, Kelkar A, Theurkauf WE. 2003. Drosophila checkpoint kinase 2 couples centrosome function and spindle assembly to genomic integrity. Cell. 113(1):87–99. doi:10.1016/S0092-8674(03)00202-2.

Ting CY, Bhatia NS, Lim JY, Goh CJ, Vasanwala RF, Ong CC, Seow WT, Yeow VK, Ting TW, Ng IS, *et al.* 2020. Further delineation of CDC45-related Meier-Gorlin syndrome with craniosynostosis and review of literature. Eur J Med Genet. 63(2):103652. doi:10.1016/j.ejmg.2019.04.009.

Tsou MF, Wang WJ, George KA, Uryu K, Stearns T, Jallepalli PV. 2009. Polo kinase and separase regulate the mitotic licensing of centriole duplication in human cells. Dev Cell. 17(3):344–354. doi:10.1016/j.devcel.2009.07.015.

Vetro A, Savasta S, Russo Raucci A, Cerqua C, Sartori G, Limongelli I, Forlino A, Maruelli S, Perucca P, Vergani D, *et al.* 2017. MCM5: a new actor in the link between DNA replication and Meier-Gorlin syndrome. Eur J Hum Genet. 25(5):646–650. doi:10.1038/ejhg.2017.5.

Wei Y, Yu L, Bowen J, Gorovsky MA, Allis CD. 1999. Phosphorylation of histone H3 is required for proper chromosome condensation and segregation. Cell. 97(1):99–109. doi:10.1016/S0092-8674(00)80718-7.

Wilhelm T, Olziersky AM, Harry D, De Sousa F, Vassal H, Eskat A, Meraldi P. 2019. Mild replication stress causes chromosome mis-segregation via premature centriole disengagement. Nat Commun. 10(1):3585. doi:10.1038/s41467-019-11584-0.

Williams BC, Goldberg ML. 1994. Determinants of Drosophila zw10 protein localization and function. J Cell Sci. 107(4):785–798. doi:10.1242/jcs.107.4.785.

Zhou FY, Waterman DP, Ashton M, Caban-Penix S, Memisoglu G, Eapen VV, Haber JE. 2024. Prolonged cell cycle arrest in response to DNA damage in yeast requires the maintenance of DNA damage signaling and the spindle assembly checkpoint. Elife. 13: RP94334. doi:10.7554/eLife.94334.

Editor: B. Calvi